Electronic Supplementary Information for

Investigating subtle 4*f* vs. 5*f* coordination differences using kinetically inert Eu(III), Tb(III), and Cm(III) complexes of a coumarin-appended 1,4,7,10-Tetraazacyclododecane-1,4,7-triacetate (DO3A) ligand

Anne Kathrine R. Junker,[a] Gauthier J.-P. Deblonde,[b] Rebecca J. Abergel[b]* and Thomas Just Sørensen[a]*

[a.] *Nano-Science Center & Department of Chemistry, University of Copenhagen, Universitetsparken 5, 2100 København Ø, Denmark*
[b.] *Chemical Sciences Division, Lawrence Berkeley National Laboratory, Berkeley, California 94720, USA.*

Table of Content

NMR and HRMS spectra of Preligand (1)

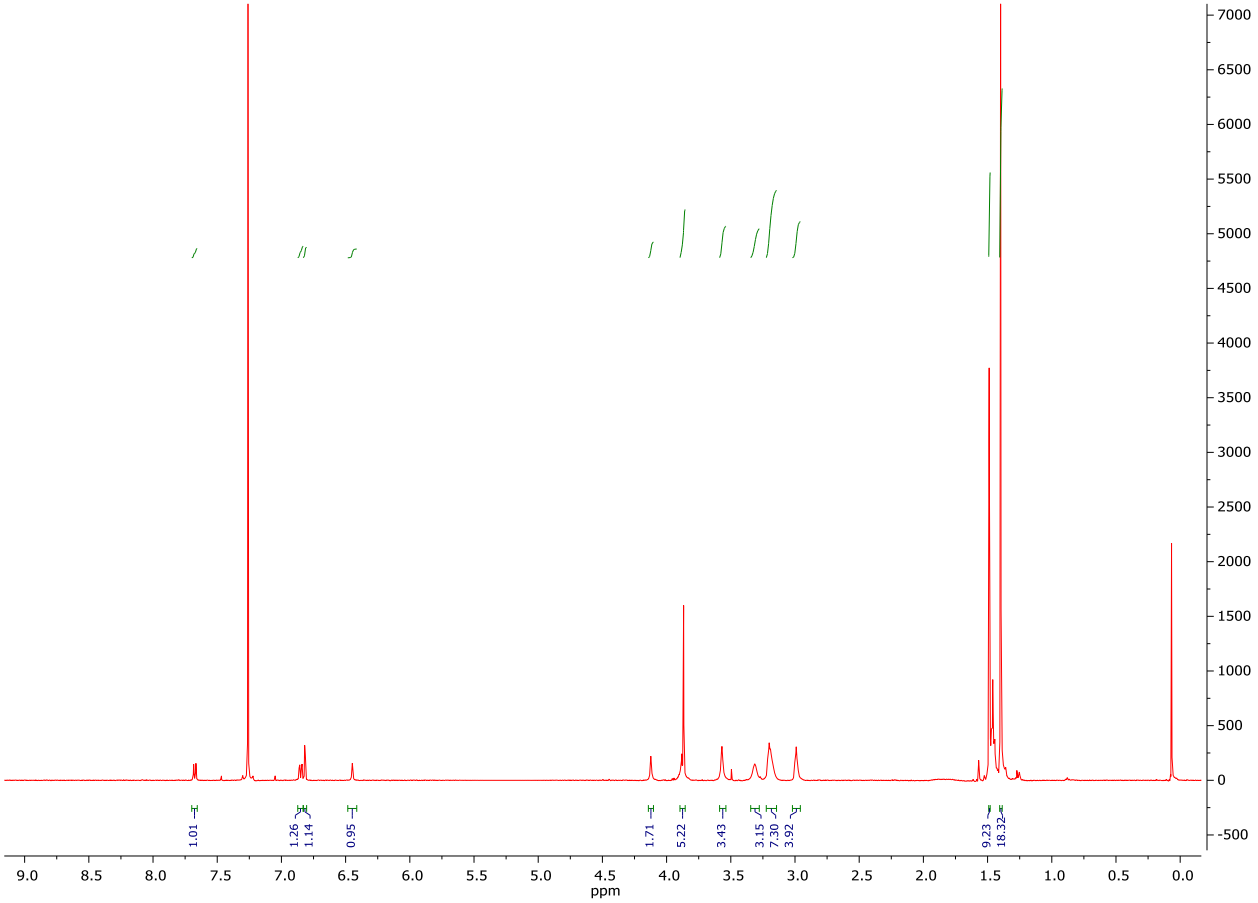

Figure S1. ^{1}H-NMR spectrum of **1** (500 MHz $CDCl_3$). Signal at 1.21 and 3.48 ppm are residual diethylether.

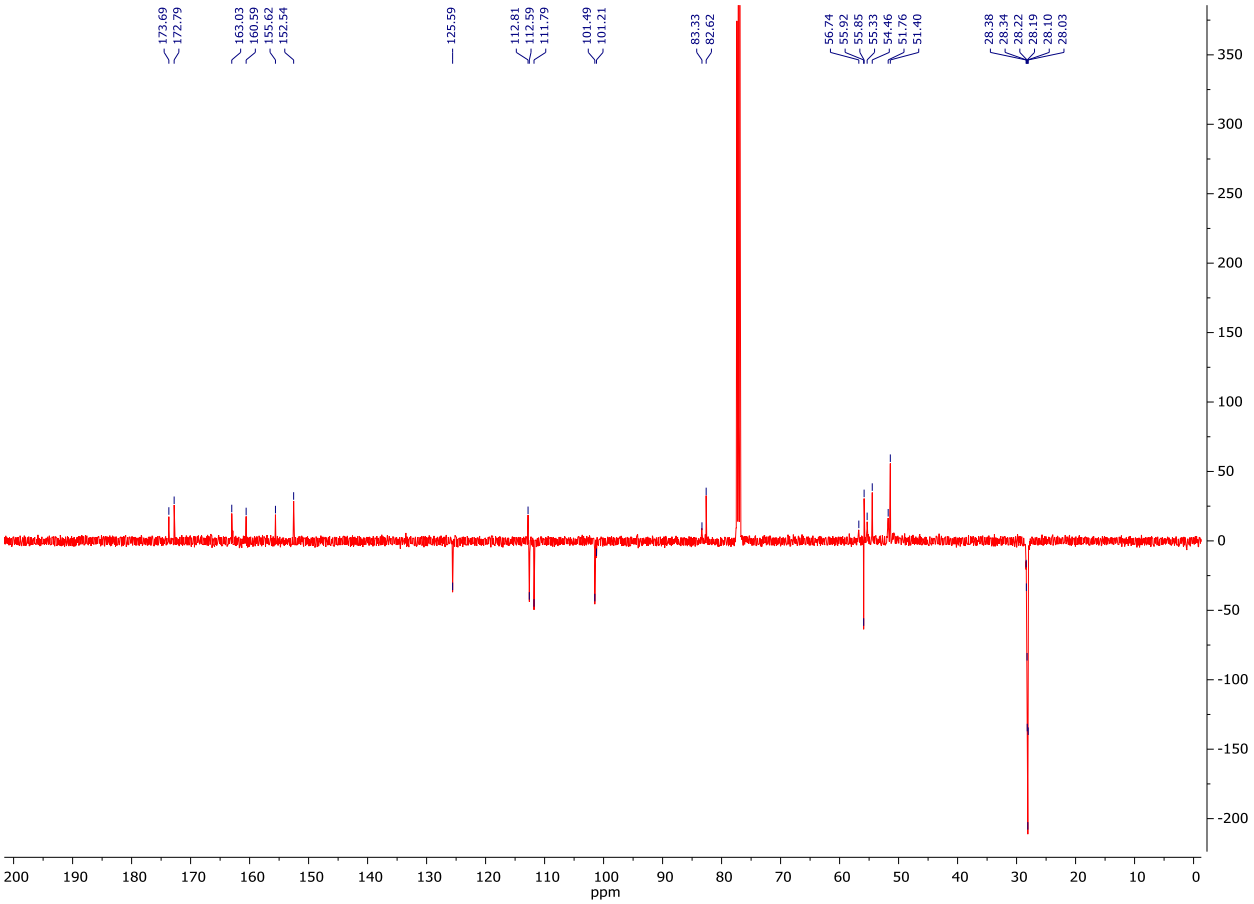

Figure S2. ^{13}C-NMR spectrum of **1** (126 MHz $CDCl_3$).

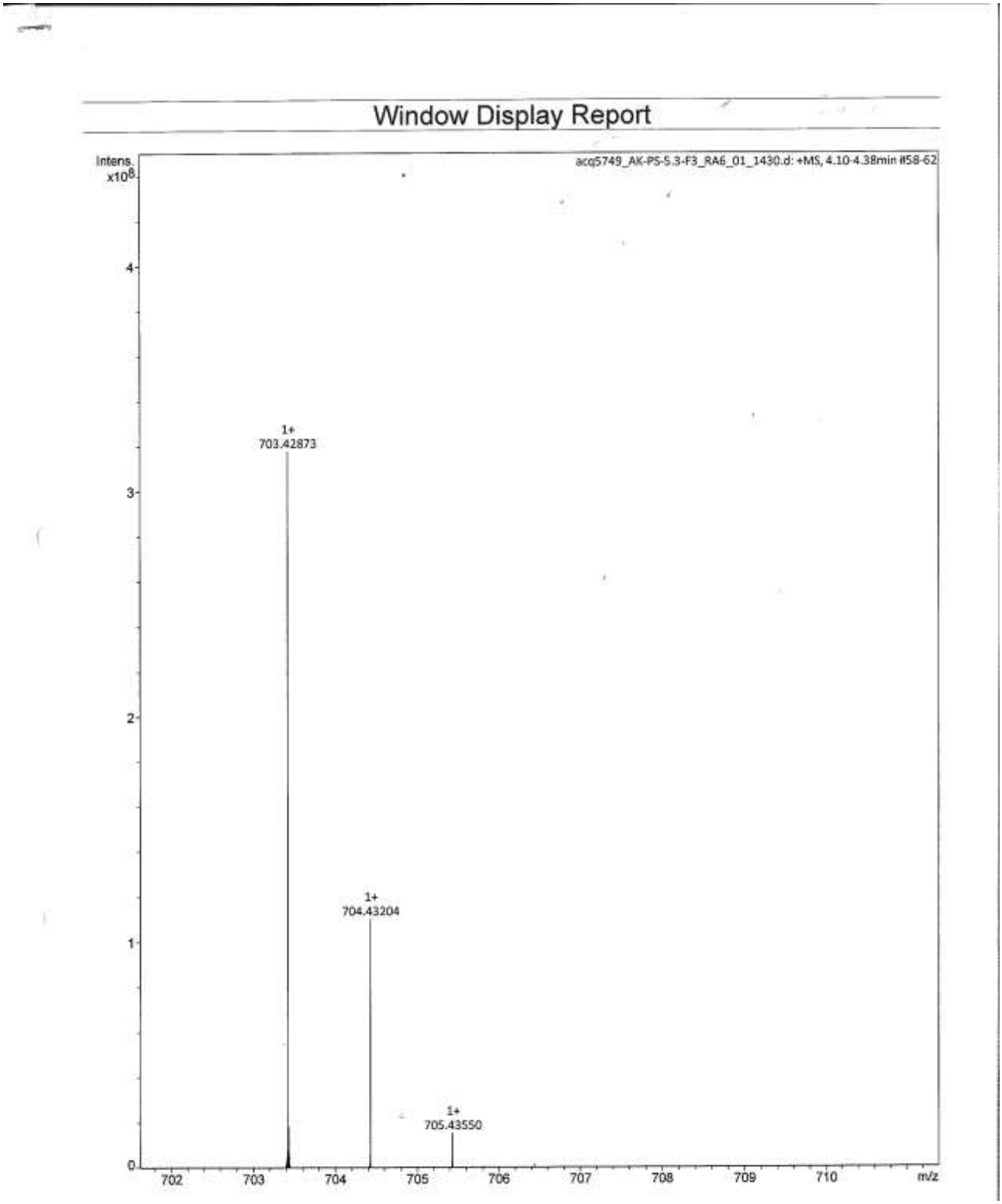

Figure S3. HRMS spectra of **1**.

NMR and HRMS spectra of Ligand (L)

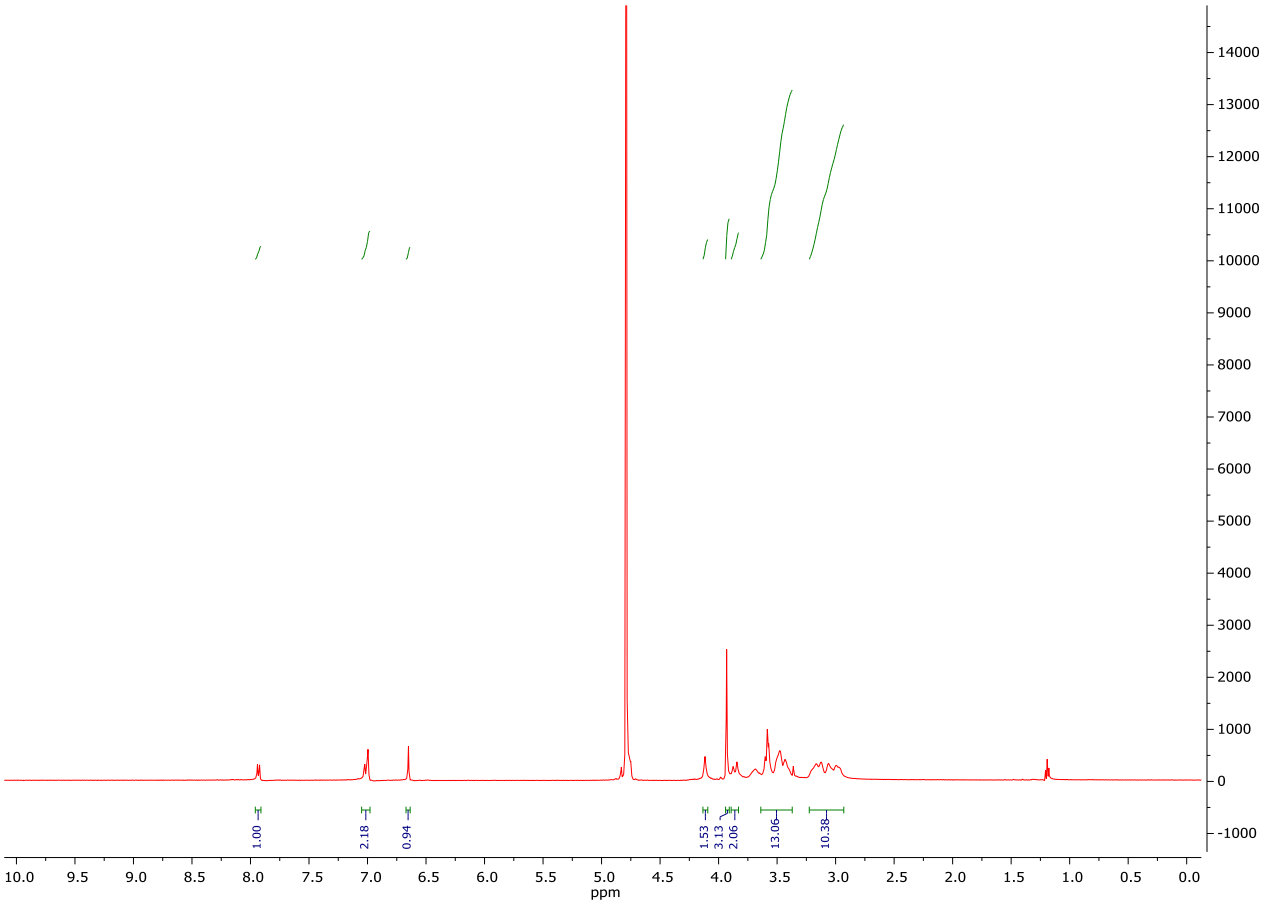

Figure S4. ^{1}H-NMR spectrum of **L** (500 MHz D_2O). Signal at 1.12 ppm residual diethylether.

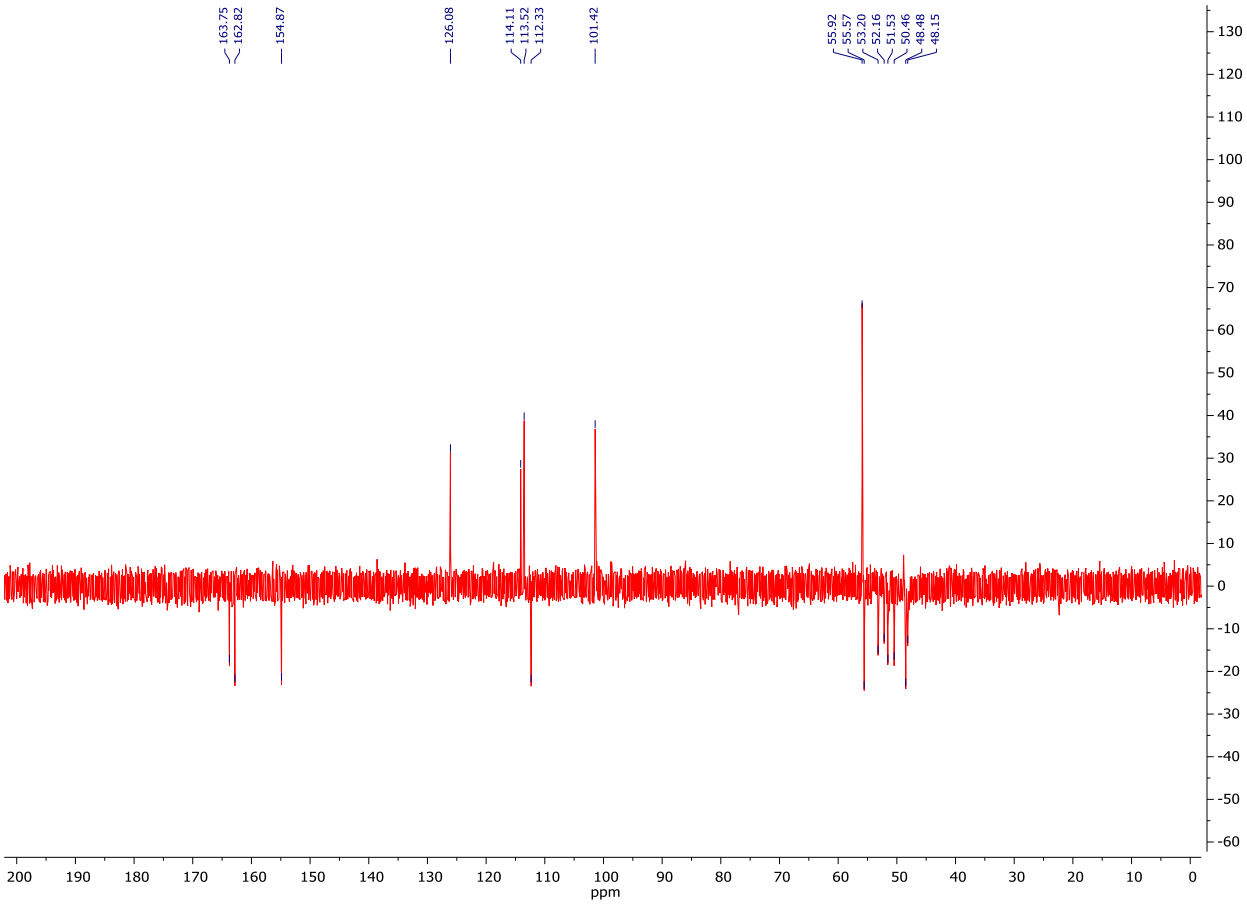

Figure S5. ^{13}C NMR spectrum of **L** (126 MHz D_2O). 4 quaternary carbon signals from the coumarin are missing.

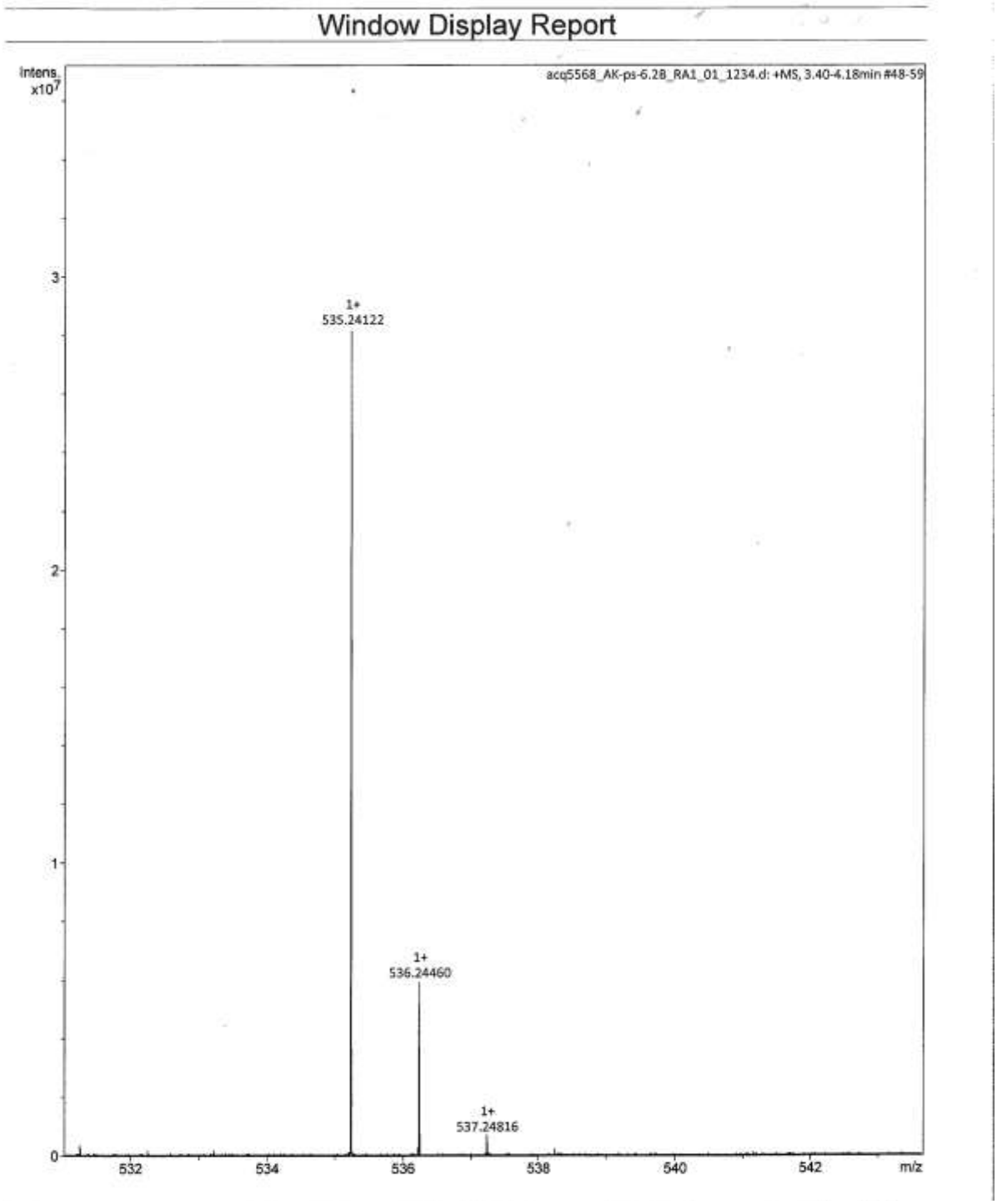

Figure S6. HRMS spectrum of **L**.

High-Resolution mass spectra of complexes

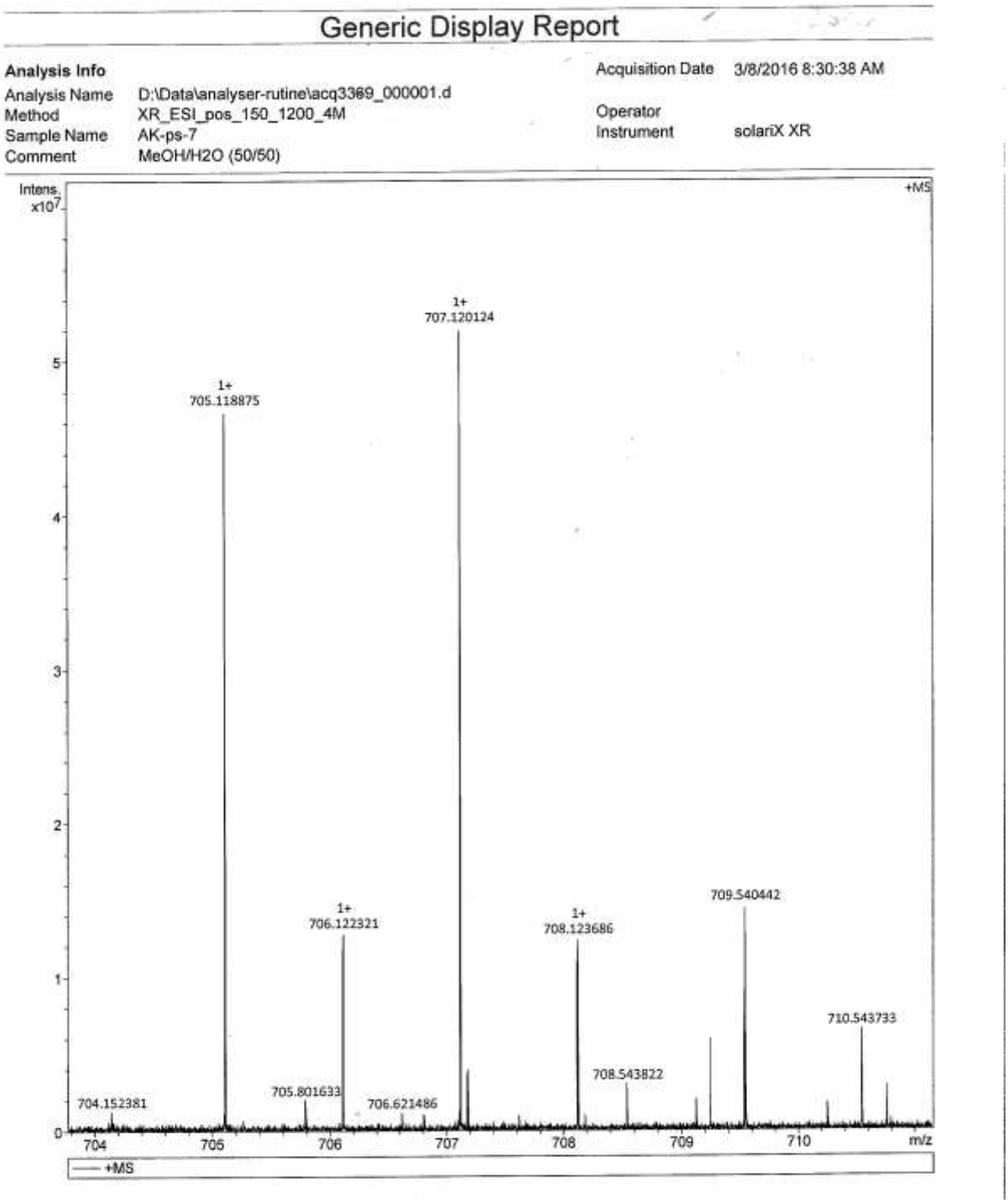

Figure S7. HRMS spectrum of **Eu**.**L**.

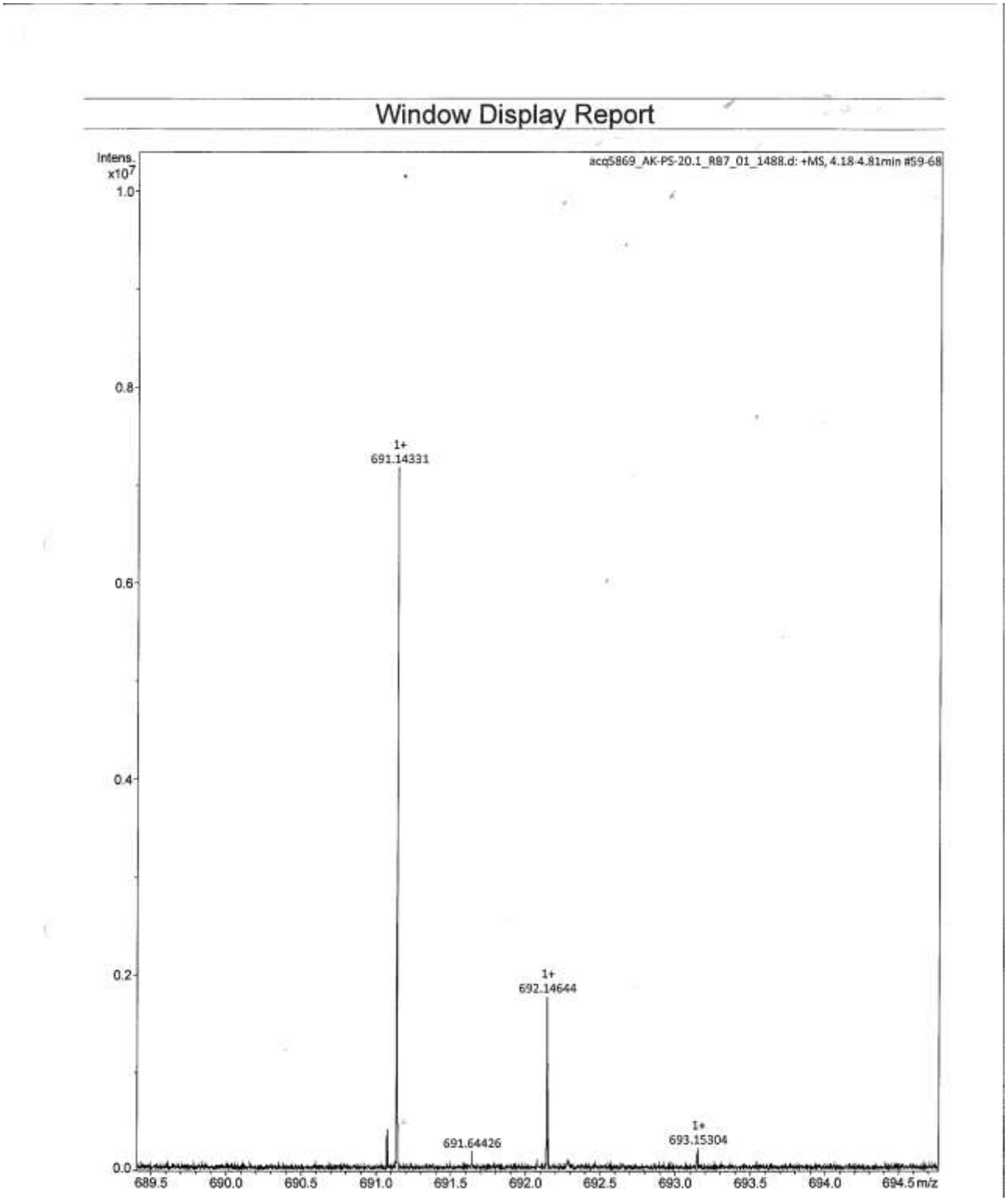

Figure S8. HRMS spectrum of **Tb**.**L**.

Spectroscopy

UV/VIS spectroscopy: All spectra were recorded on a Varian Cary 6000i double beam absorption spectrophotometer, using quartz cells of 1 cm path length for Eu.**L** and 0.01 cm for Tb.**L**, Cm.**L**. All absorbance values were corrected from the absorbance of the corresponding buffer.

Luminescence spectroscopy: All steady state, excitation and emission spectra were recorded on a HORIBA Jobin Yvon IBH FluoroLog-3 spectrofluorimeter. A sub-microsecond Xenon flashlamp (Jobin Yvon, 5000XeF) was used as the light source, with an input pulse energy (100 nF discharge capacitance) of ca. 50 mJ, yielding an optical pulse duration of less than 300 ns at full width at half maximum (FWHM). Spectral selection was achieved by passage through a double grating excitation monochromator (2.1 nm/mm dispersion, 1200 grooves/mm). Emission was monitored perpendicular to the excitation pulse; again with spectral selection. The time-gated emission spectrum of Tb.**L** was recorded on a Cary Eclipse fluorescence spectrometer with a photomultiplier tube from Agilent Technologies. For all luminescence measurements, the absorbance at the excitation wavelength and longer wavelengths was kept below 0.1 to avoid inner filter effects and intermolecular interactions. All luminescence experiments were performed in either 1 cm or 0.01 cm quartz cells. Luminescence lifetimes were determined on a HORIBA Jobin Yvon IBH FluoroLog-3 spectrofluorimeter, adapted for time-correlated single photon counting (TCSPC) and multichannel scaling (MCS) measurements. The luminescence decays were analyzed and fitted to exponential decay functions using the Origin software package.

Eu.L absorption, excitation and luminescence spectra

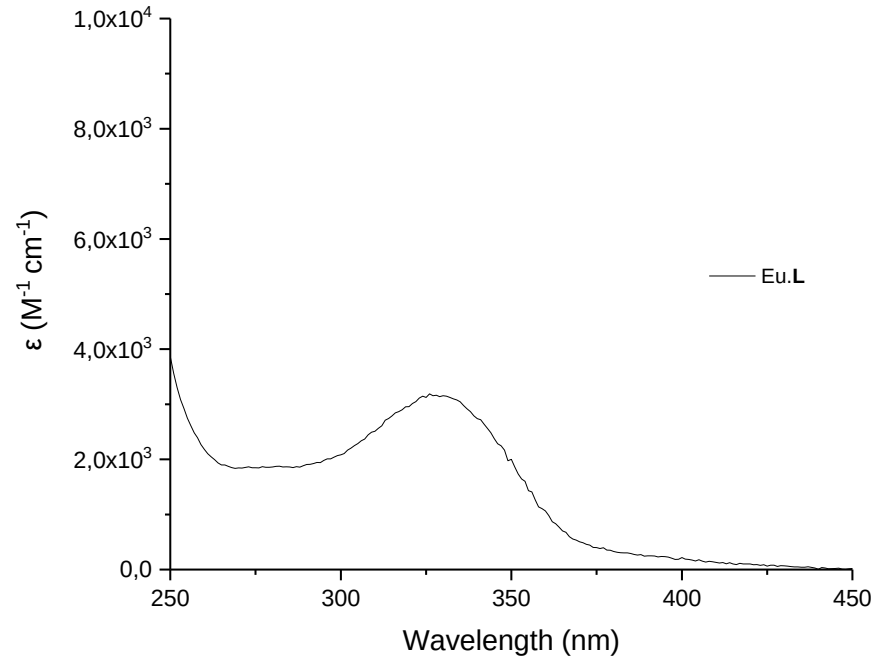

Figure S9. Absorption spectrum of Eu.**L,** 15 μM in HEPES buffer at pH 7.4.

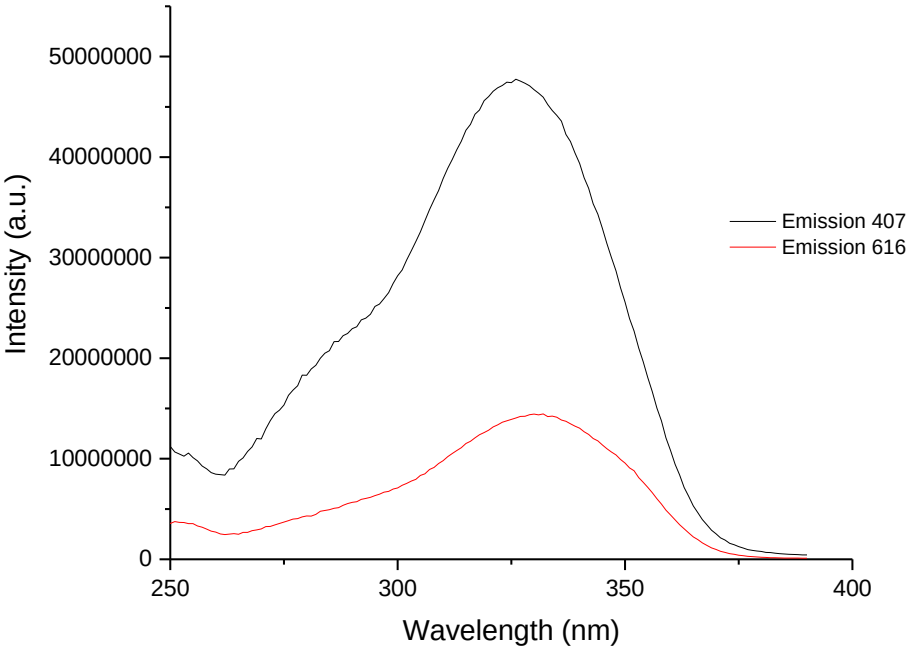

Figure S10. Excitation spectra of Eu.**L,** 15 μM in HEPES buffer at pH 7.4. Emission followed at 407 (black curve) and 616 nm (red curve), slits 3 nm (excitation) and 5 (emission).

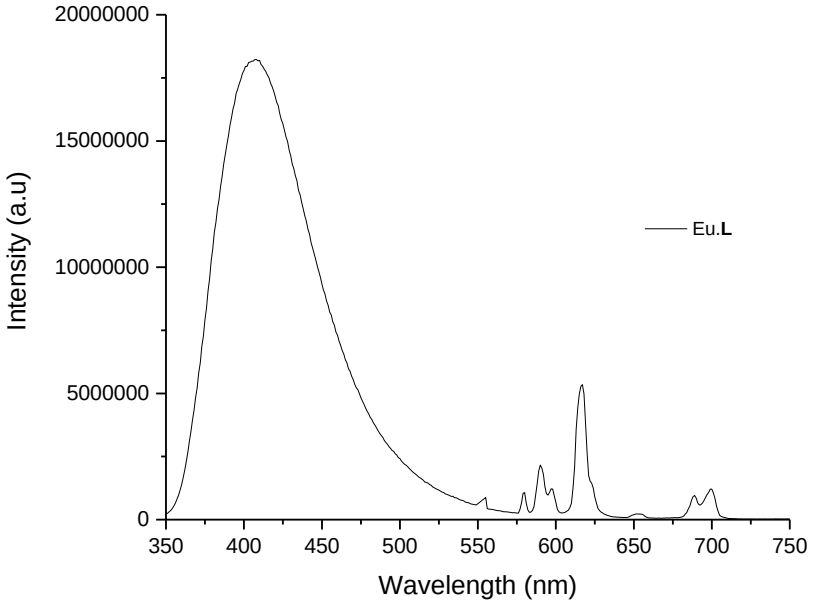

Figure S11. Emission spectrum of Eu.**L,** 15 μM in HEPES buffer at pH 7.4. Excitation at 325 nm, slits 5 nm (excitation) and 3 nm (emission).

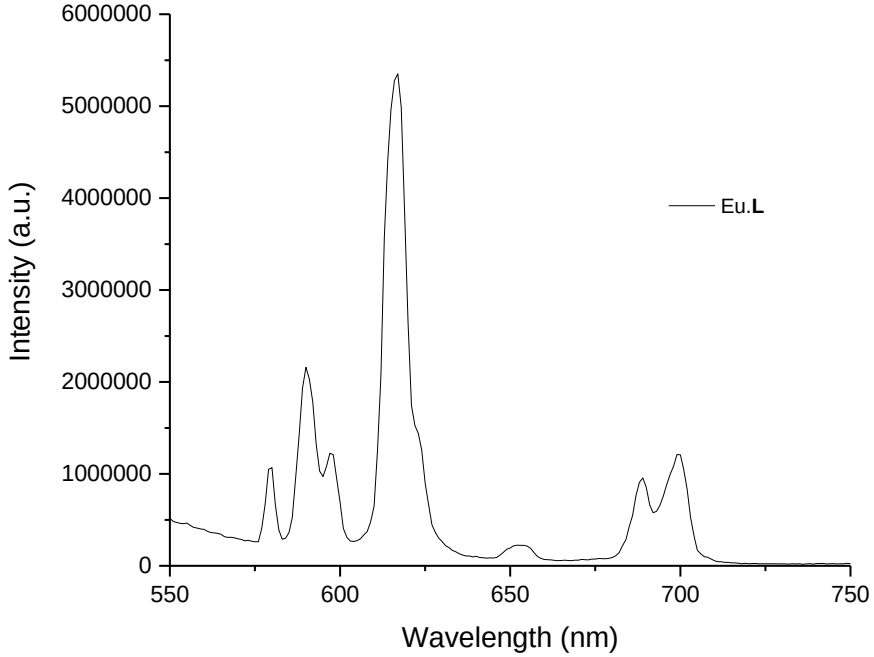

Figure S12. Zoom of emission spectrum Eu.**L**, focused on the Eu emission. Excitation at 325 nm, slits 5 nm (excitation) and 3 nm (emission).

Tb.L absorption, excitation and luminescence spectra

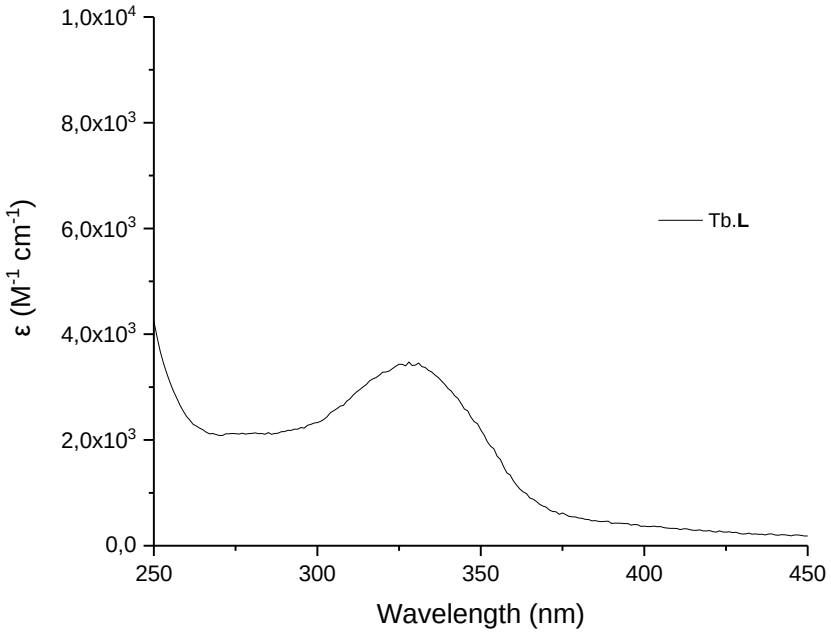

Figure S13. Absorption spectrum of Tb.**L,** 15 μM in HEPES buffer at pH 7.4.

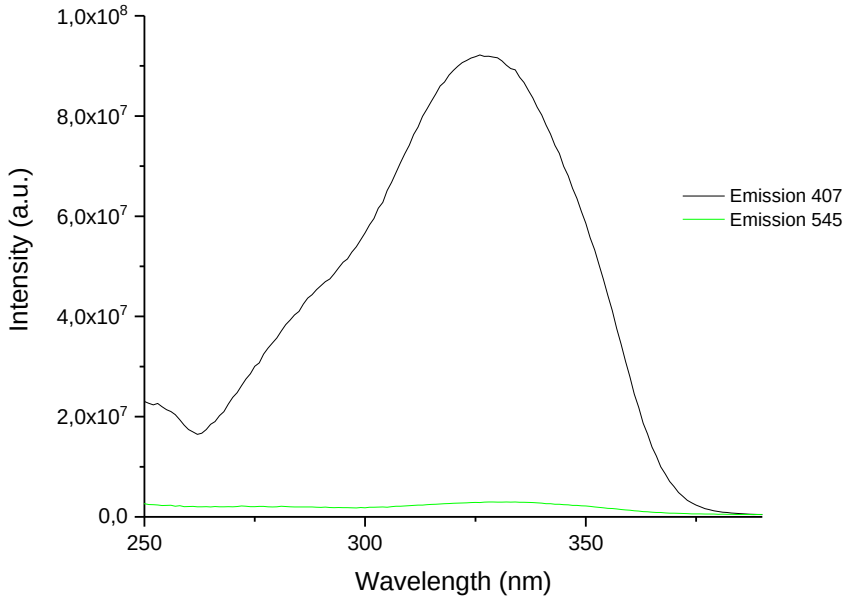

Figure S14. Excitation spectra of Tb.**L,** 15 μM in HEPES buffer at pH 7.4. Emission followed at 407 (black curve) and 545 nm (green curve), slits 3 nm (excitation) and5 nm (emission).

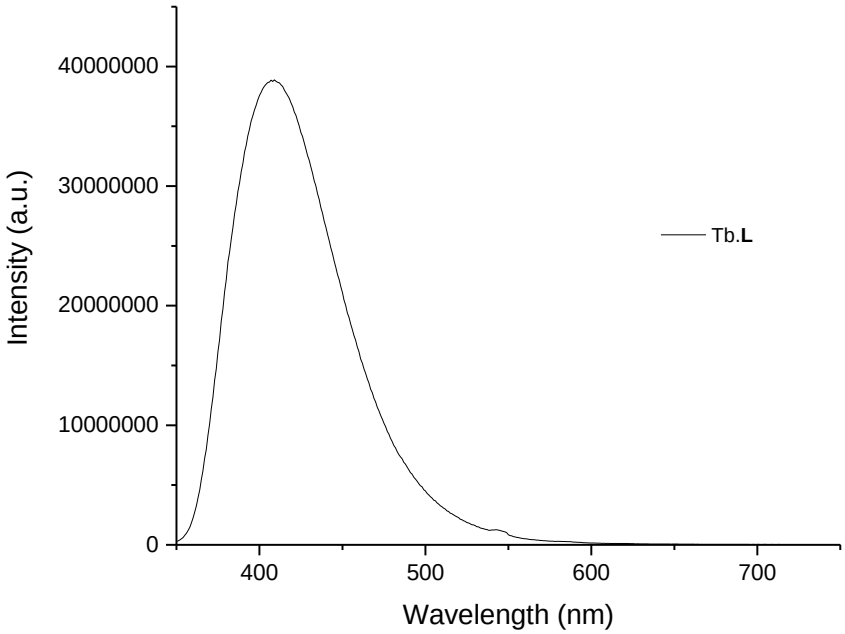

Figure S15. Emission spectrum of Tb.**L,** 15 μM in HEPES buffer at pH 7.4. Excitation at 325 nm, slits 5 nm (excitation) and 3 nm (emission).

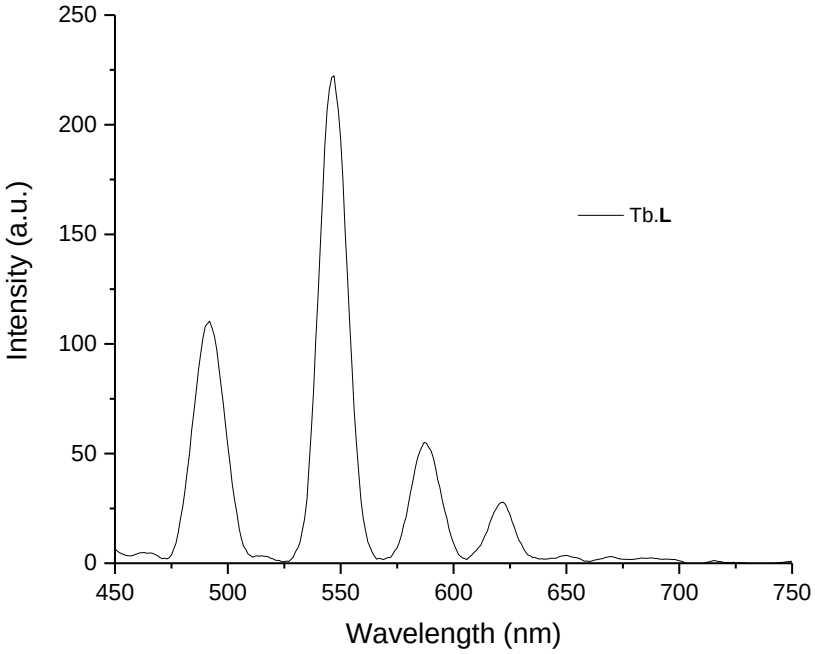

Figure S16. Time gated emission spectrum of Tb.**L,** 15 μM in HEPES buffer at pH 7.4. Excitation at 325 nm, slits 20 nm (excitation) and 20 nm (emission), total decay time 0.01 s. delay 0.2 ms, gate time 3 ms.

Cm.L absorption, excitation and luminescence spectra

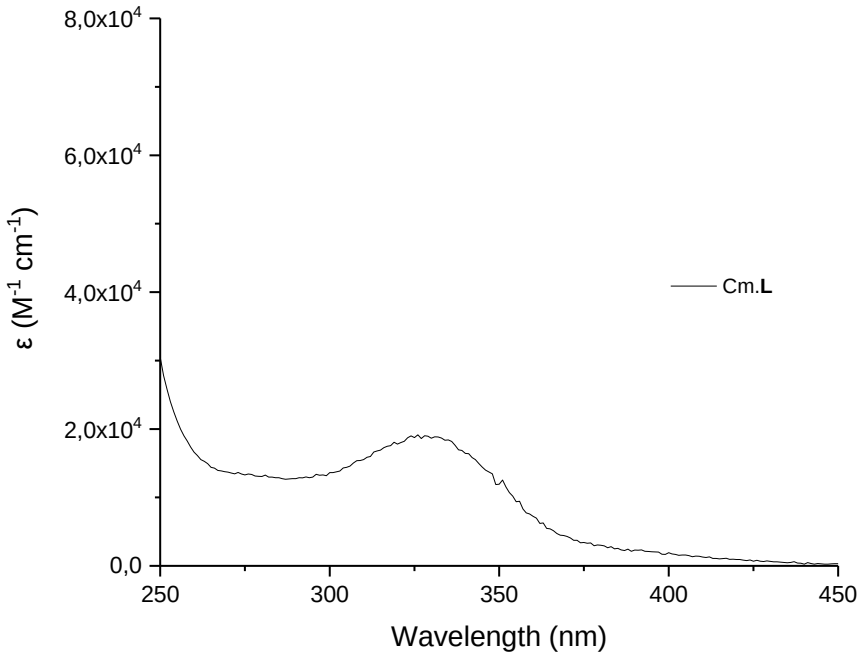

Figure S17. Absorption spectrum of Cm.**L,** 1.68 μM in HEPES buffer at pH 7.4.

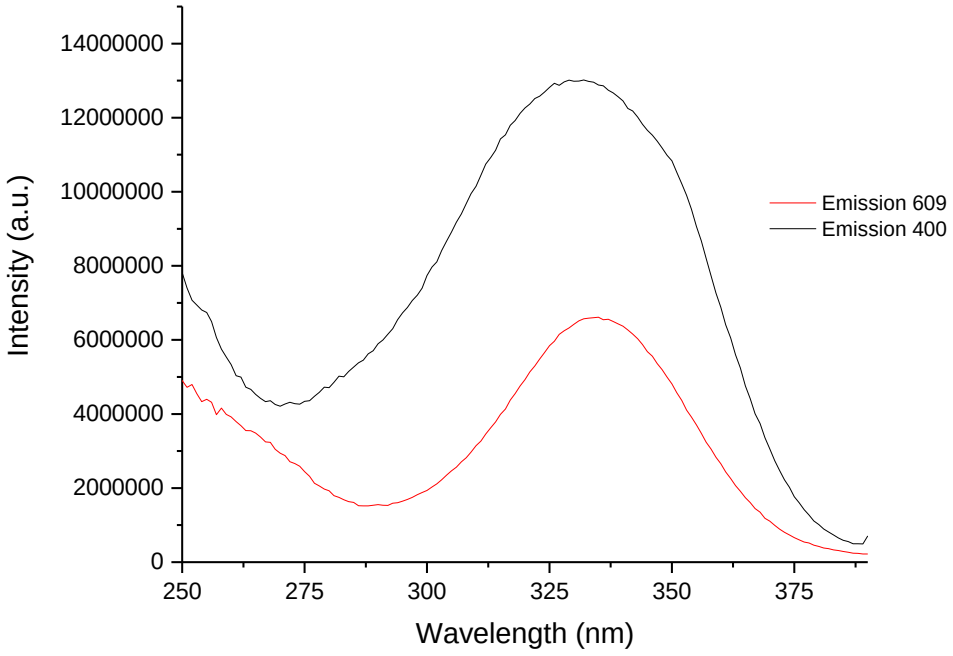

Figure S18. Excitation spectra of Cm.**L,** 1.68 μM in HEPES buffer at pH 7.4. Emission followed at 400 (black curve) and 609 nm (red curve), slits 3 nm (emission) and 5 nm (emission).

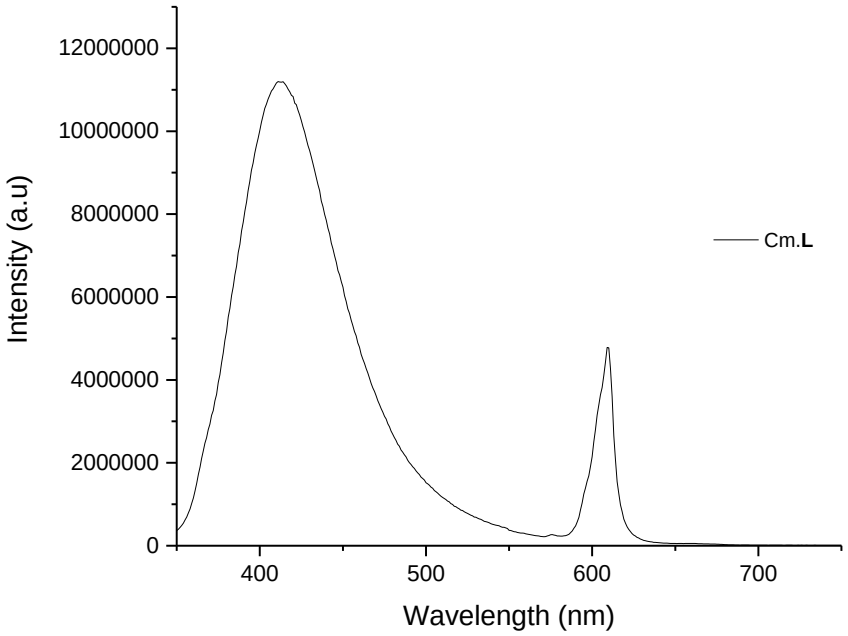

Figure S19. Emission spectra Cm.**L,** 1.68 μM in HEPES buffer at pH 7.4. Excitation at 325 nm, slits 5 nm (excitation) and 3 nm (emission).

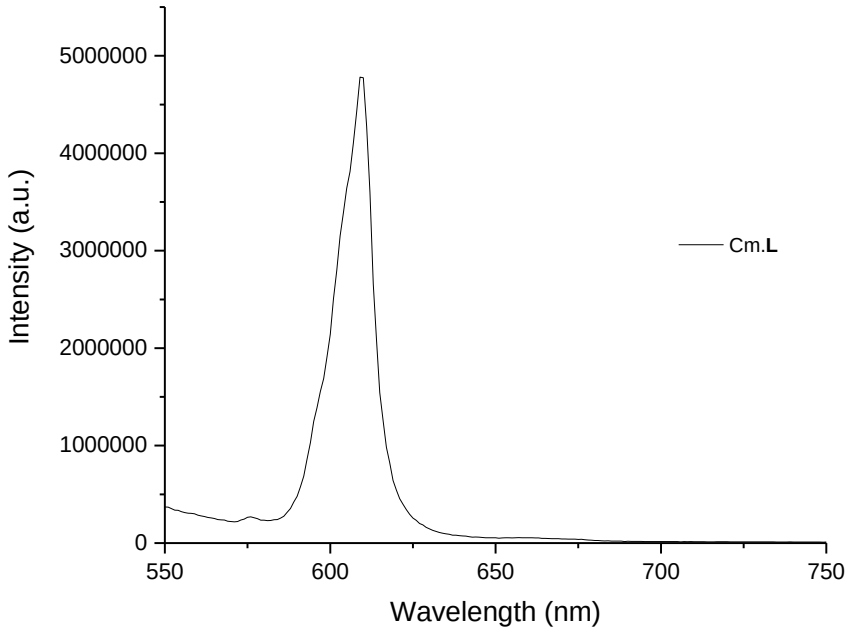

Figure S20. Zoom of emission spectrum Cm.**L**, focused on the Cm emission. Excitation at 325 nm, slits 5 nm (excitation) and 3 nm (emission).

Lifetimes

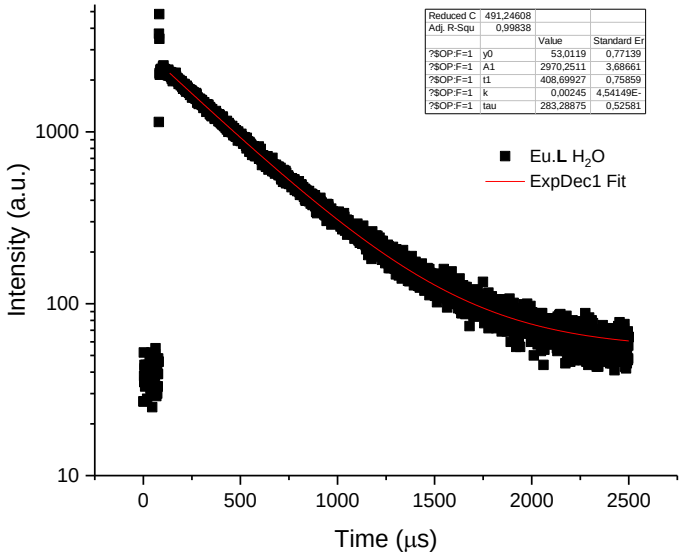

Figure S21. Time-resolved emission decay profile and fit for Eu.**L,** 15 μM (pH 7.4 in HEPES buffer), monitored at 616 nm following 325 nm light excitation.

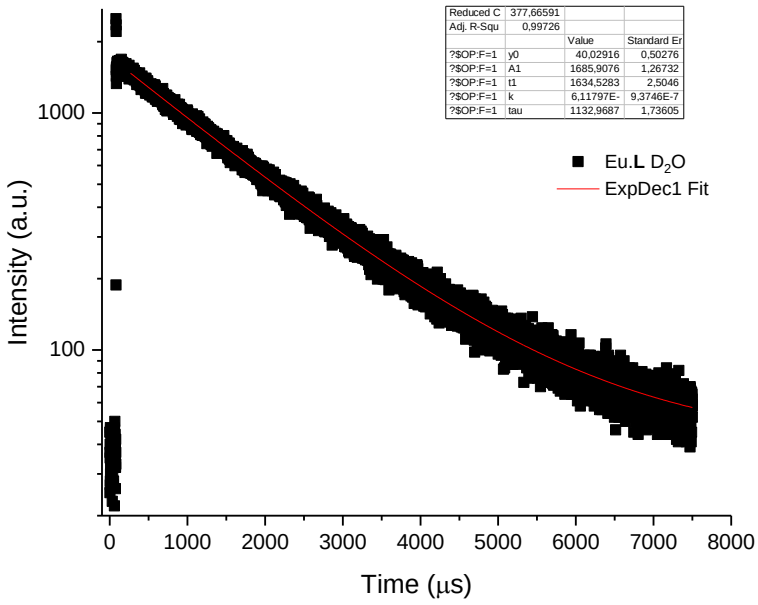

Figure S22. Time-resolved emission decay profile and fit for Eu.**L,** 15 μM (pH 7.4 in D_2O HEPES buffer), monitored at 616 nm following 325 nm light excitation.

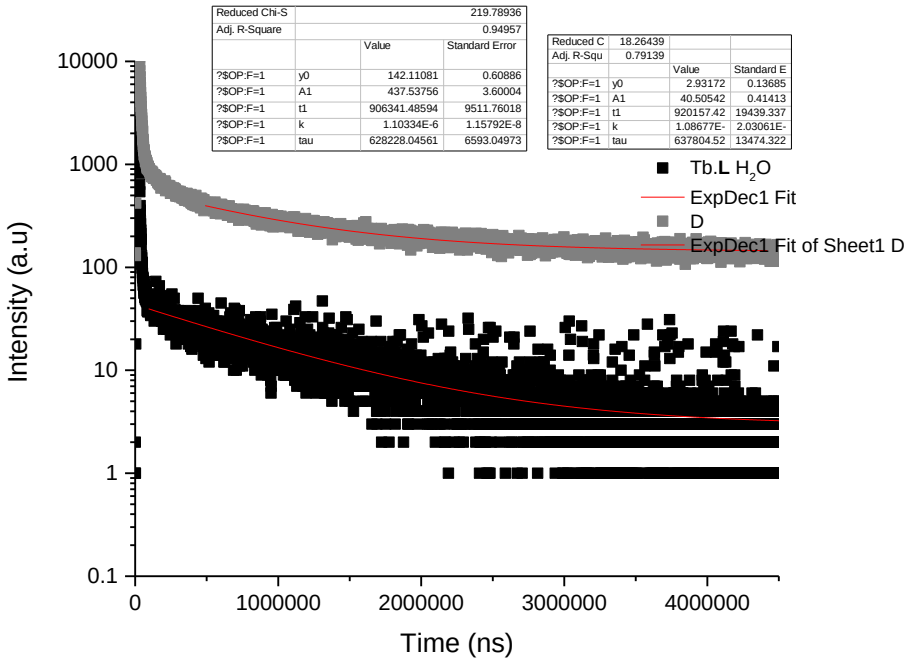

Figure S23. Time-resolved emission decay profile and fit for Tb.**L,** 15 μM(pH 7.4 in HEPES buffer), monitored at 545 nm following 325 nm light excitation. First determination (black), second determination (gray).

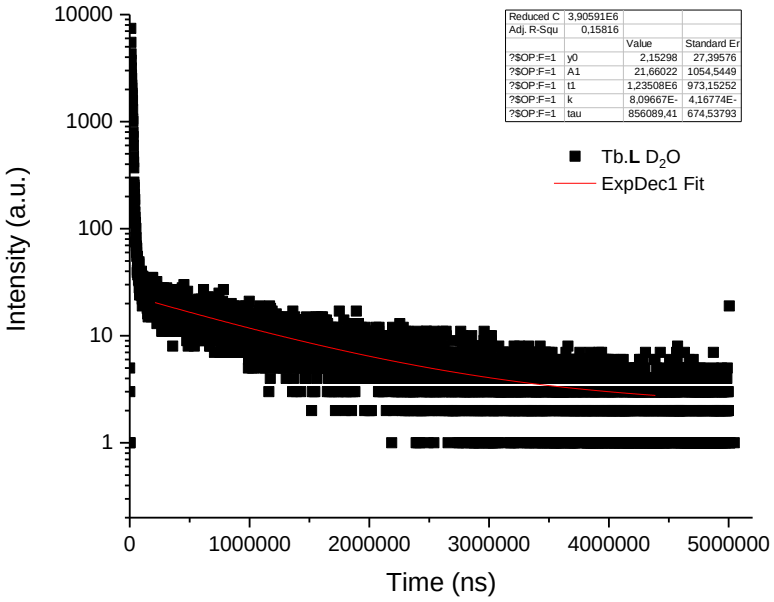

Figure S24. Time-resolved emission decay profile and fit for Tb.**L,** 15 μM (pH 7.4 in D_2O HEPES buffer), monitored at 545 nm following 325 nm light excitation.

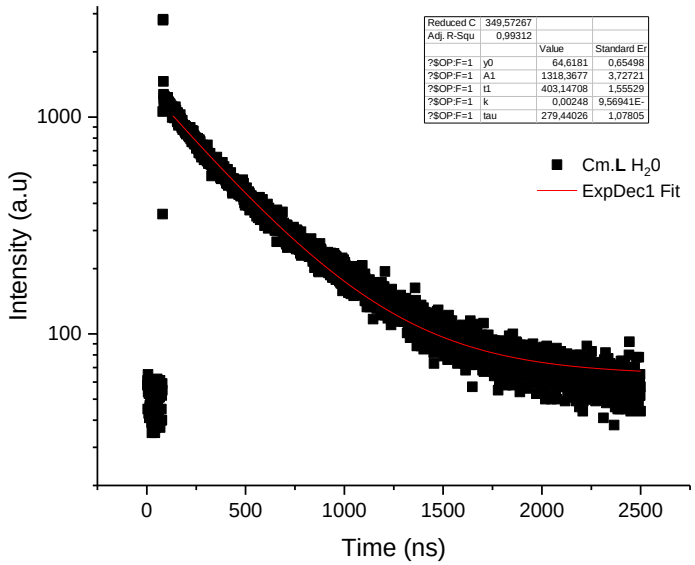

Figure S25. Time-resolved emission decay profile and fit for Cm.**L,** 1.68 μM (pH 7.4 in HEPES buffer), monitored at 610 nm following 325 nm light excitation.

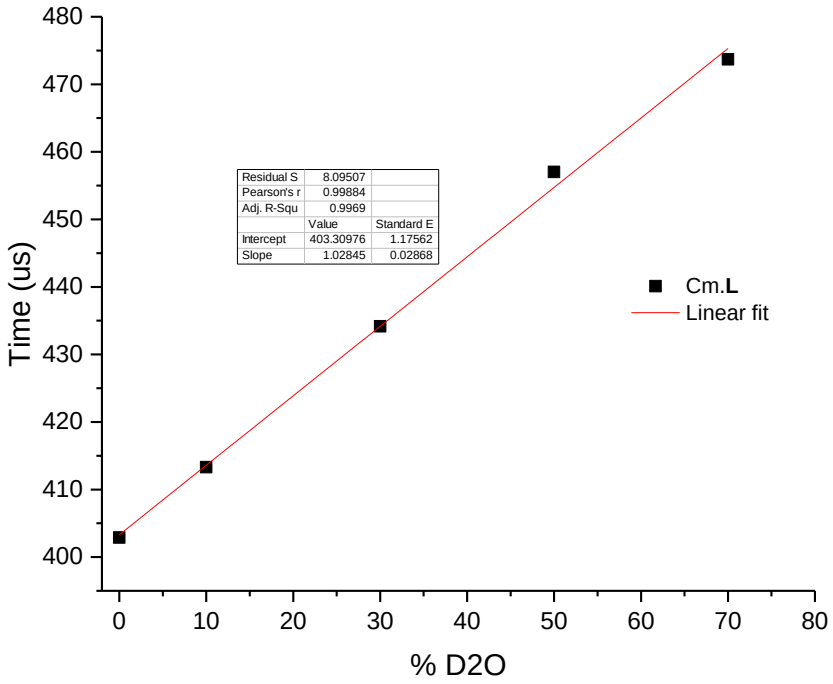

Figure S26. Emission decay profile observed for Cm.**L** with increasing volumic ratio of D_2O. The data was fitted to a linear decay to determine the associated lifetime.

Quantum yield data

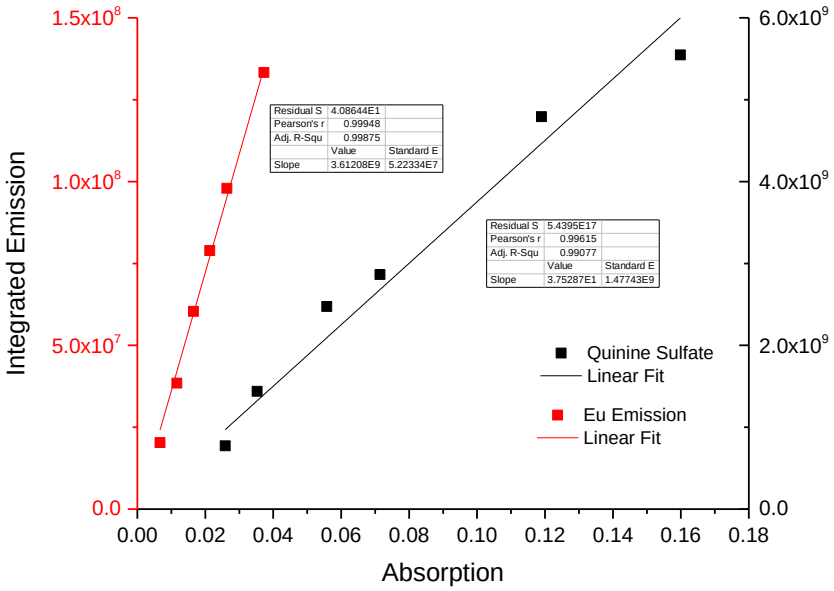

Figure S27. Quantum yield determination for the Eu(III) centred emission from Eu.**L** (575-725 nm). pH 7.4 (0.1 M HEPES Buffer). The red line is a linear fit of the data for the sample and the black line is a linear fit of the data for the reference quinine sulfate.

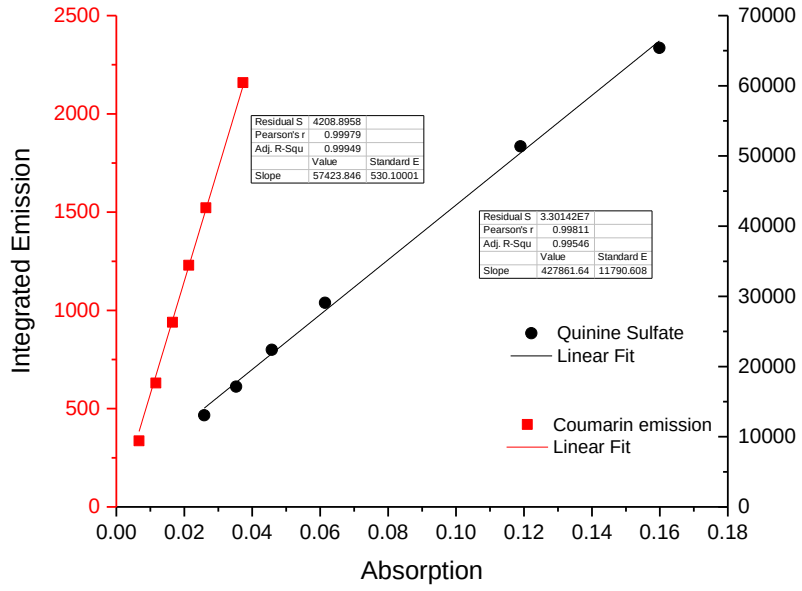

Figure S28. Quantum yield determination for the coumarin emission from Eu.**L** at pH 7.4 (0.1 M HEPES Buffer). The red line is a linear fit of the data for the sample and the black line is a linear fit of the data for the reference quinine sulfate.

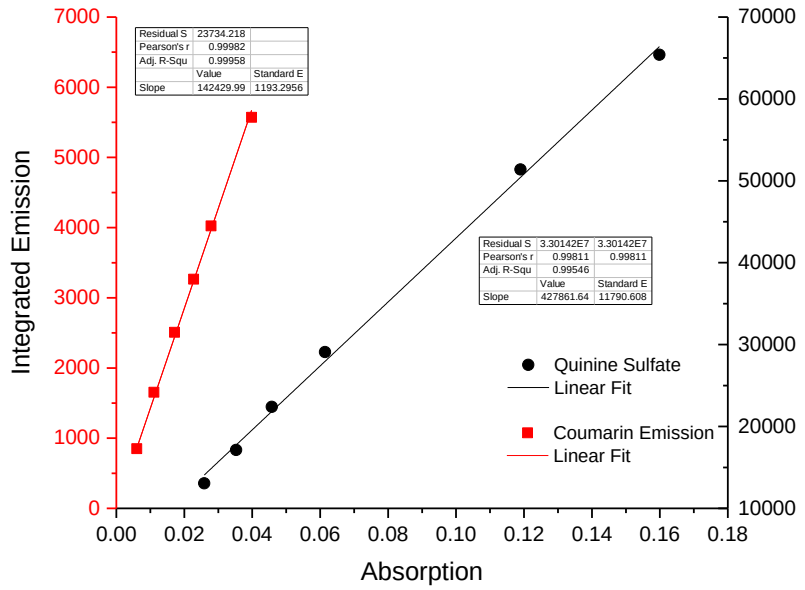

Figure S29. Quantum yield determination for the coumarin emission from Tb.**L** at pH 7.4 (0.1 M HEPES Buffer). The red line is a linear fit of the data for the sample and the black line is a linear fit of the data for the reference quinine sulfate.

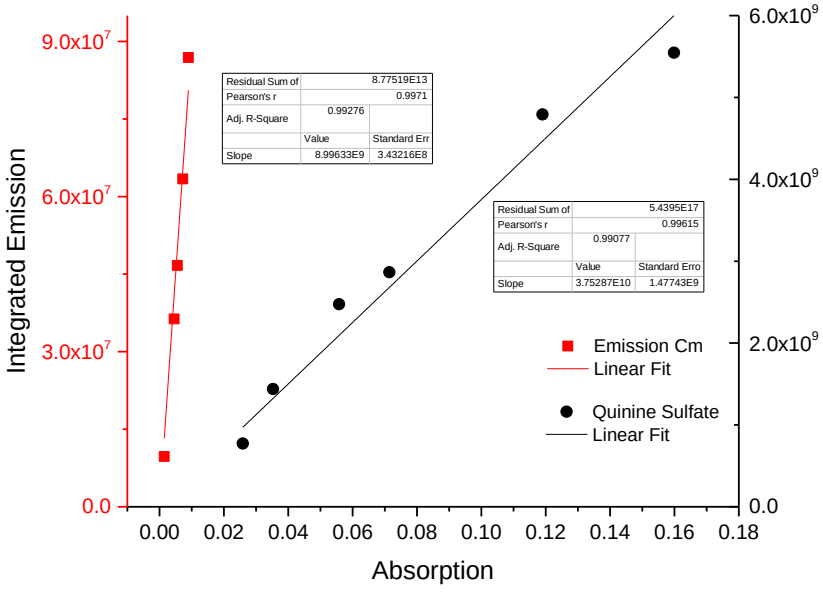

Figure S30. Quantum yield determination for Cm(III) centred emission from Cm.**L**. pH 7.4 (0.1 M HEPES Buffer). The red line is a linear fit of the data for the sample and the black line is a linear fit of the data for the reference quinine sulfate.

Spectrofluorimetric Competition Batch Titrations with EDTA or DTPA

Series of aqueous samples containing a fixed concentration of Eu.**L** (1.4 μM) and a varying amount of ligand competitor (0 to 10 equivalents of EDTA or 0 to 500 equivalents of DTPA) were prepared in KCl 0.1 M/HEPES buffer 10 mM.
For the first attempt to challenge Eu.**L** with EDTA, the samples were equilibrated in a thermostatic shaker at 60 °C (4 days), and then at 25 °C (3 days) until equilibrium was reached and measurements were stable (7 days). At the concentration used in these experiments, Eu(III) luminescence from Eu.**L** can be easily observed whereas Eu(III) luminescence from Eu.EDTA was too weak to be observed. Hence, a complete disappearance of the Eu(III) emission was expected if the Eu(III) was complexed by EDTA at the expense of **L**. As shown in Figure S27, no significant change was observed in the steady state emission spectra of the samples indicating that Eu(III) remained bound to **L**.

The second attempt used DTPA as challenging ligand since the Eu.DTPA complex is more stable that its EDTA counterpart. All samples were sealed in glass vials and equilibrated in a thermostatic shaker at 60 °C (4 days), and 25 °C (3 days) until equilibrium was reached and measurements were stable (7 days). The emission spectrum of each solution was measured using a 0.1 cm quartz cell. A drop in the emission intensity (about a 5-fold decrease) of the Eu(III) centered emission from Eu.**L** was expected in the case of a ligand exchange between and **L** and DTPA due to the lower brightness of the Eu.DTPA complex. As shown in Figure S28, no significant change was observed in the steady state emission spectra of the samples indicating that the Eu.**L** complex is too inert to be challenged by DPTA, even using 500 equivalents.

1. Series Eu.**L** vs EDTA

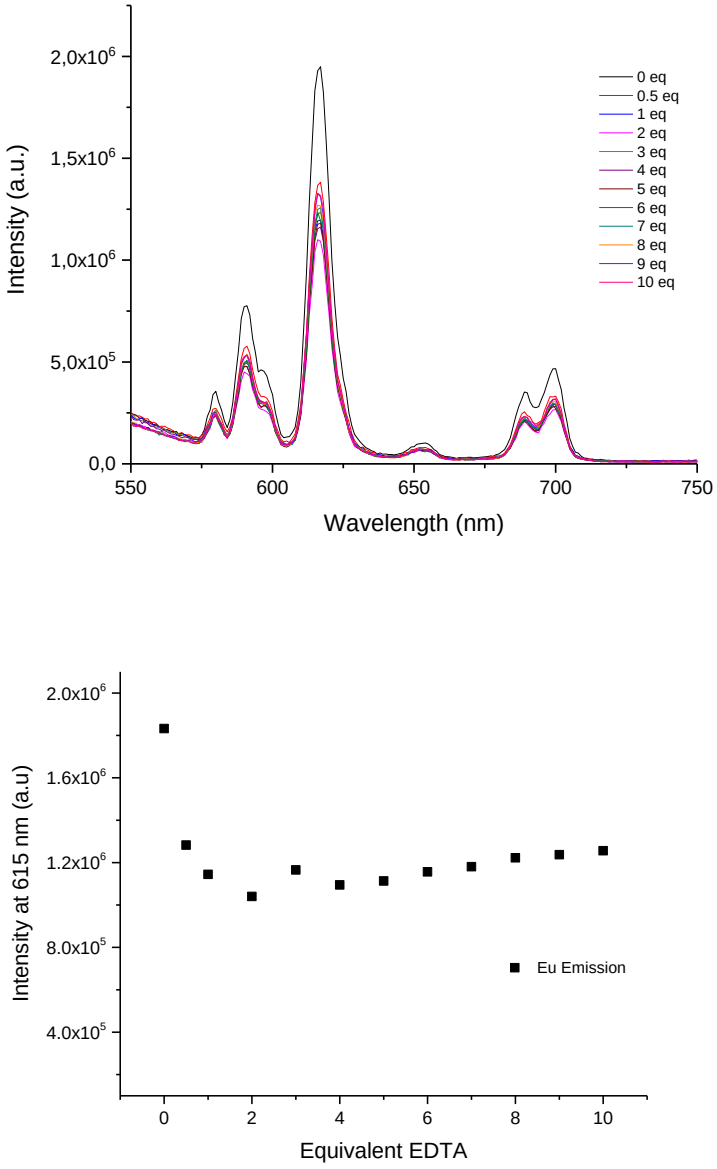

Figure S31. Top: Spectrofluorimetric competition titration of Eu.**L** against EDTA ([Eu.**L**] = 1.4 μM, [EDTA] from 0 to 13 μM, KCl 10 mM, 0.1 M HEPES, pH 7.4, 25 °C, exc = 325 nm) Bottom: change in emission intensity at 615 nm as a function of equivalents of competitor added.

2. Series Eu.**L** vs DTPA

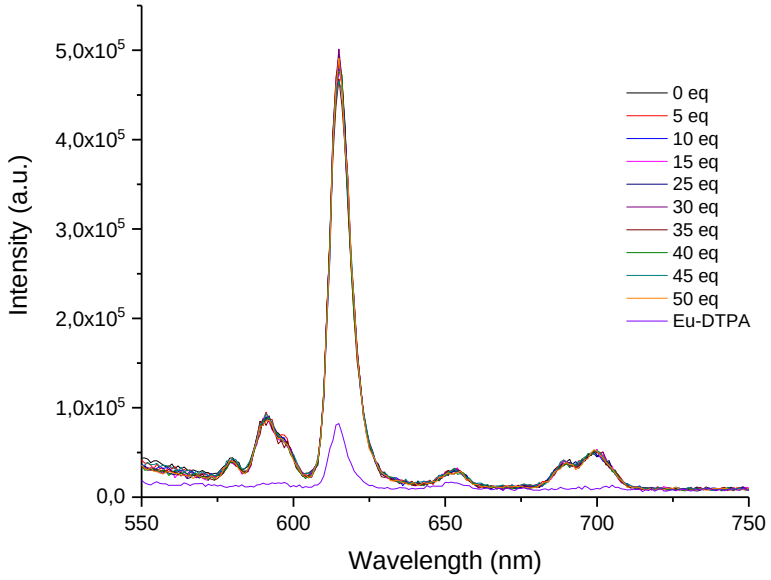

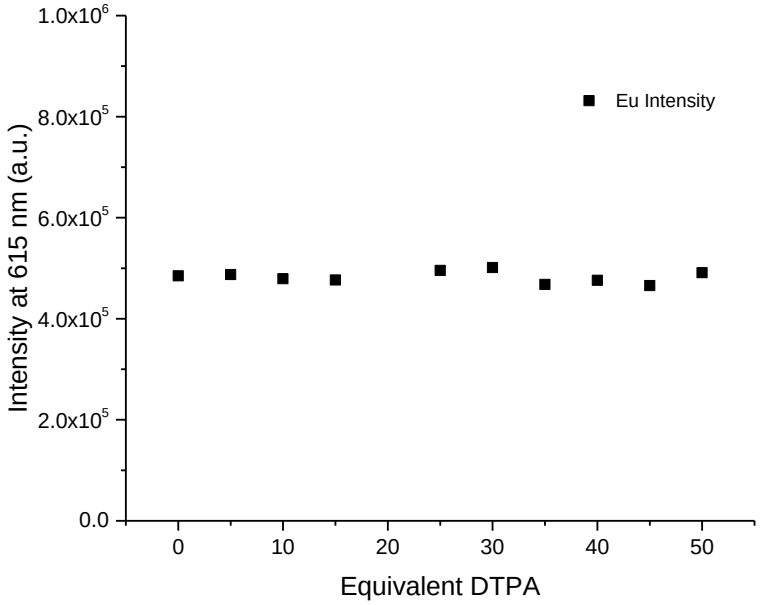

Figure S32. Top: Spectrofluorimetric competition titration of Eu.**L** against DTPA ([Eu.**L**] = 1.4 μM, [DTPA] from 0 to 70 μM, KCl 0.1 M, 10 mM HEPES, pH 7.4, 25 °C, exc = 325 nm). Bottom: change in emission intensity at 615 nm as a dunction of equivalents of competitor added.

2. Series Eu.**L** vs DTPA

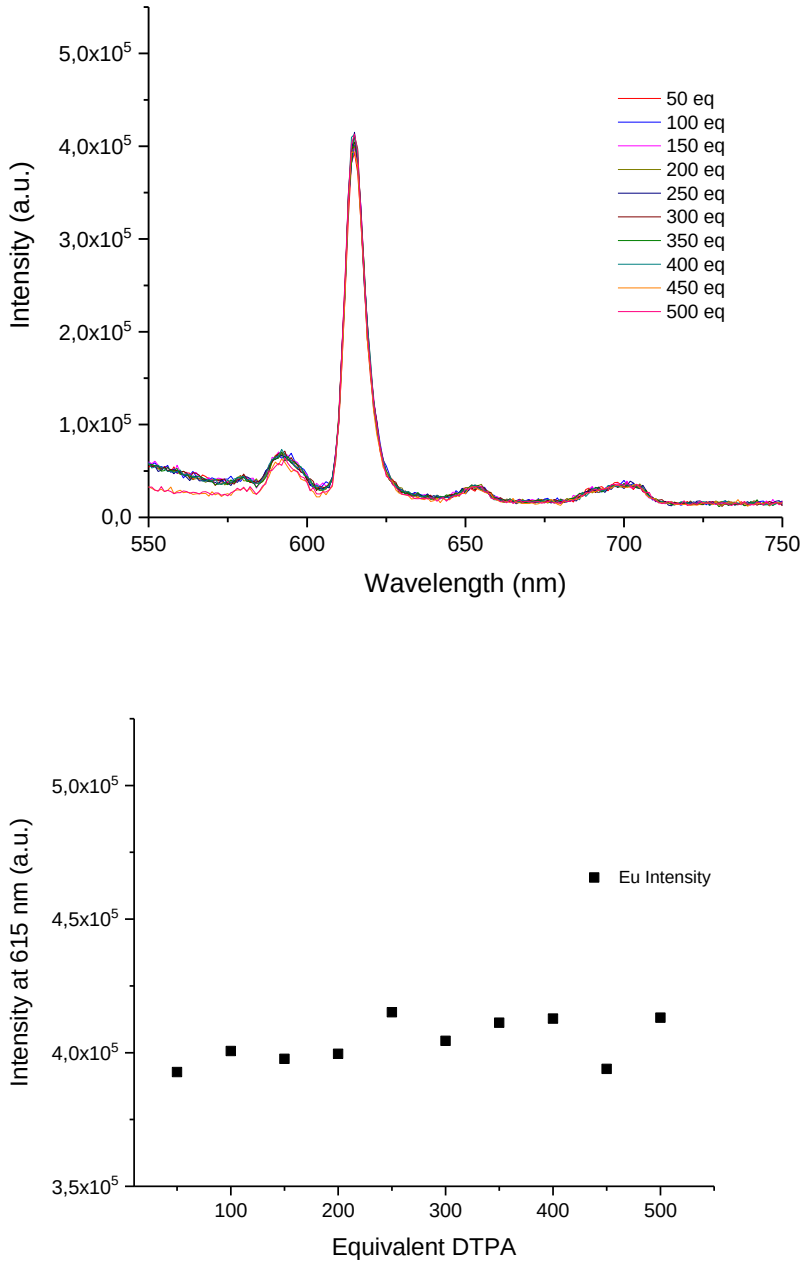

Figure S33. Top: Spectrofluorimetric competition titration of Eu.**L** against DTPA ([Eu.**L**] = 1.4 μM, [DTPA] from 0 to 700 μM, KCl 0.1 M, 10 mM HEPES, pH 7.4, 25 °C, exc = 325 nm). Bottom: change in emission intensity at 615 nm as a function of equivalents of competitor added.

Spectrofluorimetric Competition Batch Titrations with 3,4,3-LI-(HOPO)

Series of aqueous samples containing a fixed concentration of M.**L** (1.4 μM of Eu.**L** or 1.2 μM of Tb.**L or** 0.11 μM of Cm.**L**) and a varying amount of ligand competitor (0 to 50 equivalents of 3,4,3-LI(1,2-HOPO) prepared in KCl 0.1 M/HEPES buffer 10 mM. All samples were equilibrated in a thermostatic shaker at 60 °C (4 days), and 25 °C (3 days) until equilibrium was reached and measurements were stable (7 days). The emission spectrum of each solution was measured using a 0.1 cm quartz cell. In this case, an increase in the emission intensity from Eu(III), Tb(III), or Cm(III) was expected since the complexes of 3,4,3-LI(1,2-HOPO) are brighter that the corresponding complexes with **L**. Changes in the emission features (*i.e.* slight shift of the emission bands and changes in the emission line ratio) was also expected if the M.**L** complexes were in equilibrium with their 3,4,3-LI(1,2-HOPO) analogues. 3,4,3-LI(1,2-HOPO) was found to be strong enough to displace Eu(III), Tb(III), and Cm(III) from their complexes with L, as displayed in the figures S31, S33, and S35.

Data Treatment. All thermodynamic data sets were imported into the refinement program *HypSpec* and analyzed by nonlinear least-squares refinement. All equilibrium constants were defined as cumulative formation constants, β_{mlh} according to equation (2), where the metal and ligand are designed as M and L, respectively.

$$mM + lL + hH \rightleftharpoons [M_m L_l H_h]\ ;\ \beta_{mlh} = \frac{[M_m L_l H_h]}{[M]^m [L]^l [H]^h} \qquad \text{(S2)}$$

All metal and ligand concentrations were held at estimated values determined from the volume of standardized stock solutions. The emission spectra of the complexes were recorded. The refinements of the overall formation constants included the literature values for the protonation constants in each case and the metal hydrolysis products, the equilibrium constants of which was fixed to the literature values. The entire procedure (sample preparation, equilibration, spectrofluorimetric measurements, and data treatment) was, at least, duplicate for each metal-ligand system.

1. Series Eu.**L**:

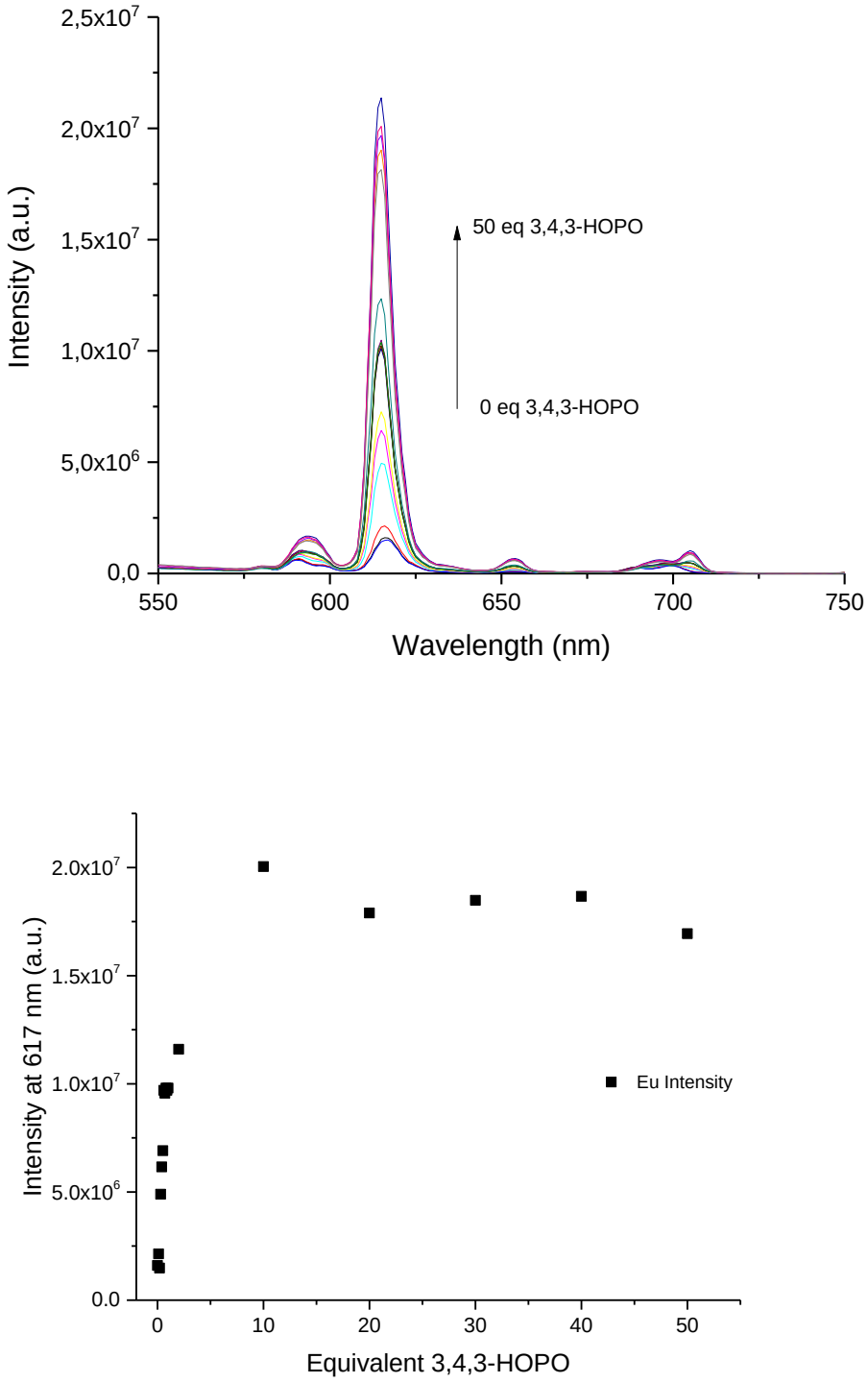

Figure S34. Top: Spectrofluorimetric competition titration of Eu.**L** (1. Series) against 3,4,3-LI(HOPO) ([Eu.**L**] = 1.4 µM, [HOPO] from 0 to 70 µM, KCl 0.1 M, 10 mM HEPES, pH 7.4, 25 °C, exc = 325 nm). Bottom: change in emission intensity at 617 nm as a function of equivalents of competitor added.

2. Series Eu**L**:

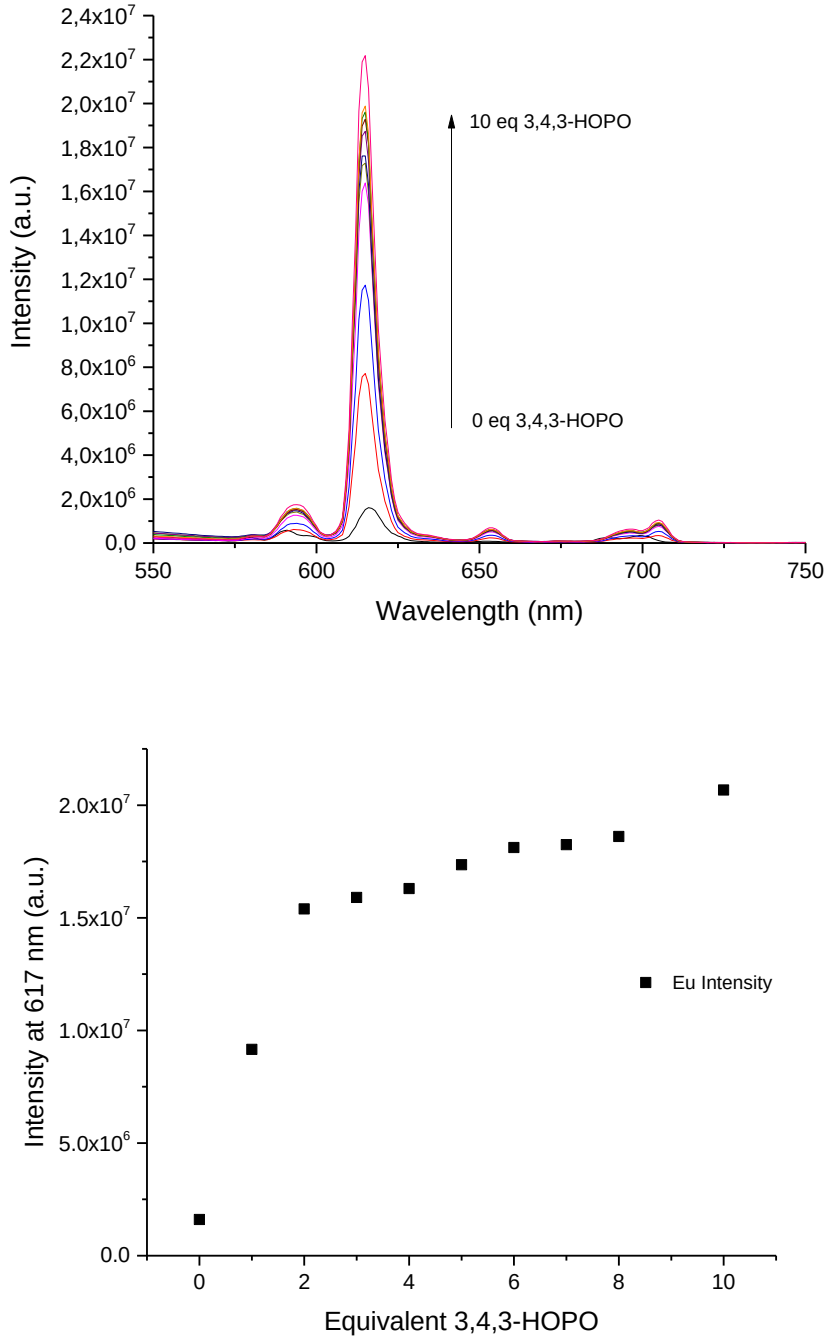

Figure S35. Top: Spectrofluorimetric competition titration of Eu.**L** (2. Series) against 3,4,3-LI(HOPO) ([Eu.**L**] = 1.4 µM, [HOPO] from 0 to 14 µM, KCl 0.1 M, 10 mM HEPES, pH 7.4, 25 °C, exc = 325 nm). Bottom: change in emission intensity at 617 nm as a function of equivalents of competitor added.

3. Series Eu.**L**:

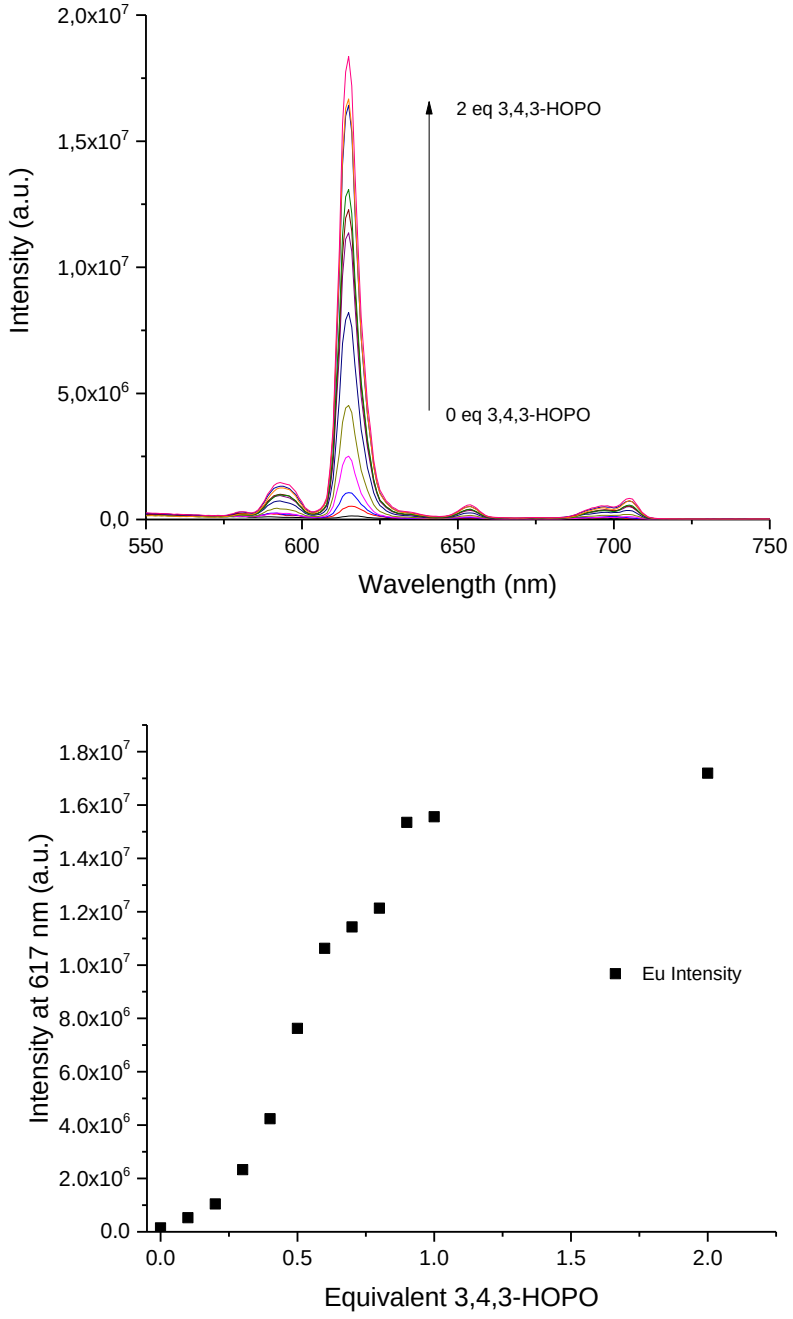

Figure S36. Top: Example of batch spectrofluorimetric competition titration of Eu.**L** against 3,4,3-LI(HOPO) ([Eu.**L**] = 1.4 µM, [HOPO] from 0 to 3µM, KCl 0.1 M, 10 mM HEPES, pH 7.4, 25 °C, exc = 325 nm). Bottom: change in emission intensity at 617 nm as a function of equivalents of competitor added.

1. Series Tb.**L:**

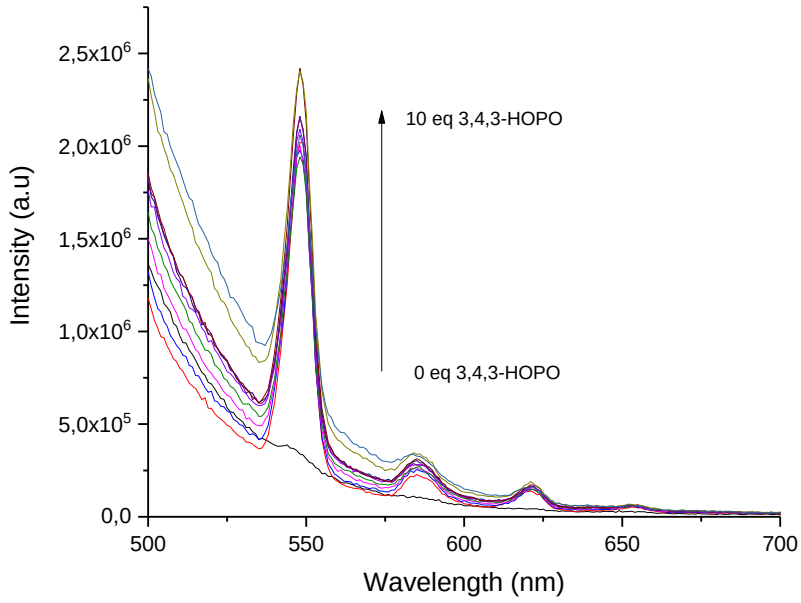

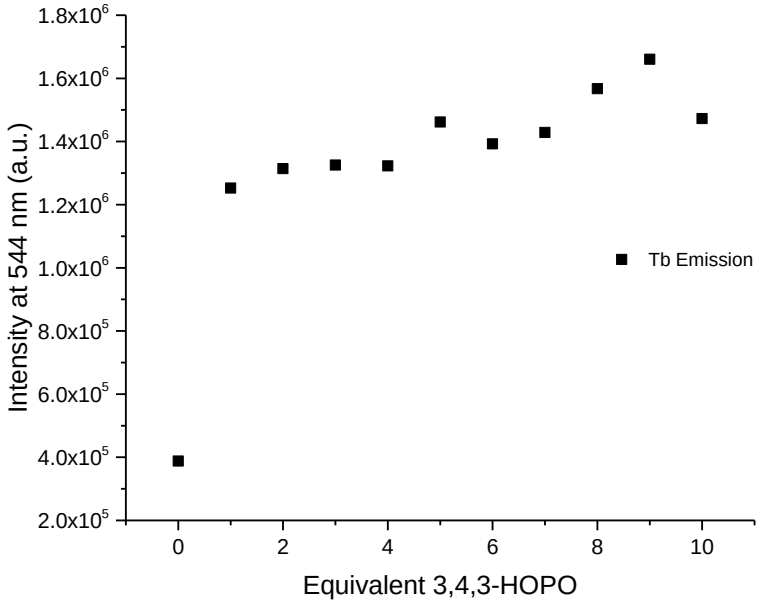

Figure S37. Top: Spectrofluorimetric competition titration of Tb.**L** against 3,4,3-LI(HOPO) ([Tb.**L**] = 1.2 µM, [HOPO] from 0 to 12 µM, KCl 0.1 M, 10 mM HEPES, pH 7.4, 25 °C, exc = 325 nm). Bottom: change in emission intensity at 544 nm as a function of equivalents of competitor added.

2. Series Tb.**L:**

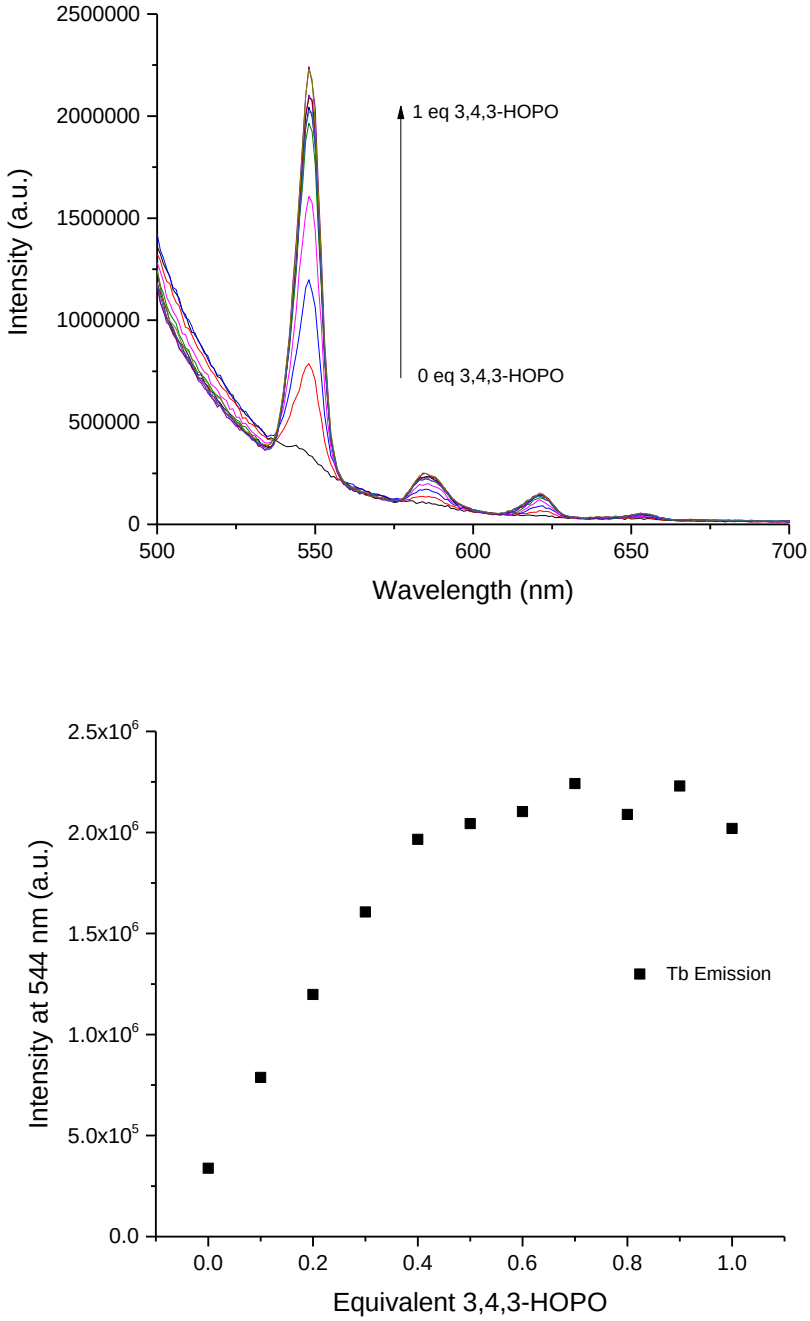

Figure S38. Top: Example of batch spectrofluorimetric competition titration of Tb.**L** against 3,4,3-LI(HOPO) ([Tb.**L**] = 1.2 μM, [HOPO] from 0 to 1.2 μM, KCl 0.1 M, 10 mM HEPES, pH 7.4, 25 °C, exc = 325 nm). Bottom: change in emission intensity at 544 nm as a function of equivalents of competitor added.

1. Series Cm.**L:**

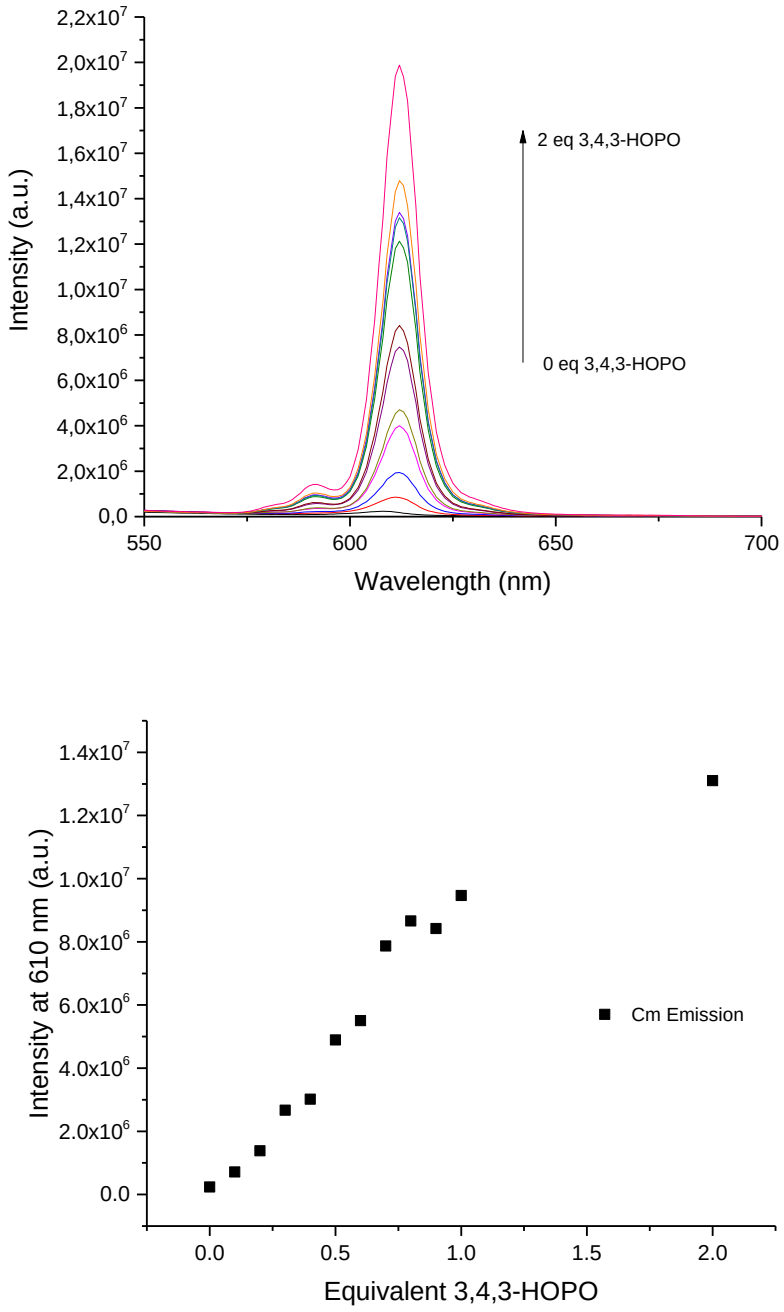

Figure S39. Top: Example of batch spectrofluorimetric competition titration of Cm.**L** (Series 1) against 3,4,3-LI(HOPO) ([Cm.**L**] = 0.11 μM, [HOPO] from 0 to 0.2 μM, KCl 0.1 M, 10 mM HEPES, pH 7.4, 25 °C, exc = 325 nm). Bottom: change in emission intensity at 610 nm as a function of equivalents of competitor added.

2. Series Cm.**L**:

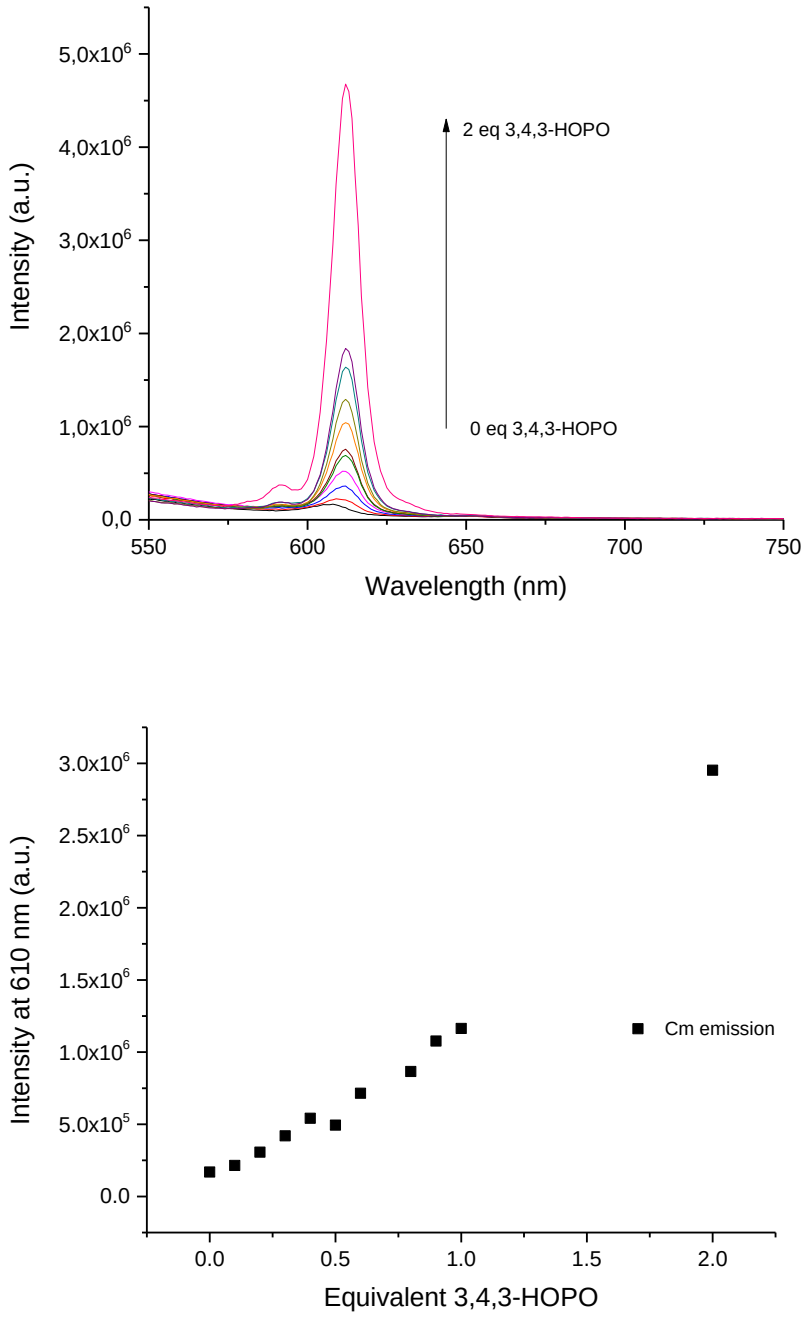

Figure S40. Top: Spectrofluorimetric competition titration of Cm.**L** (Series 2) against 3,4,3-LI(HOPO) ([Cm.**L**] = 0.11 µM, [HOPO] from 0 to 0.2 µM, KCl 0.1 M, 10 mM HEPES, pH 7.4, 25 °C, exc = 325 nm). Bottom: change in emission intensity at 610 nm as a function of equivalents of competitor added.

Fits from Spectrofluorimetric Competition Batch Titrations with 3,4,3-LI-(HOPO)

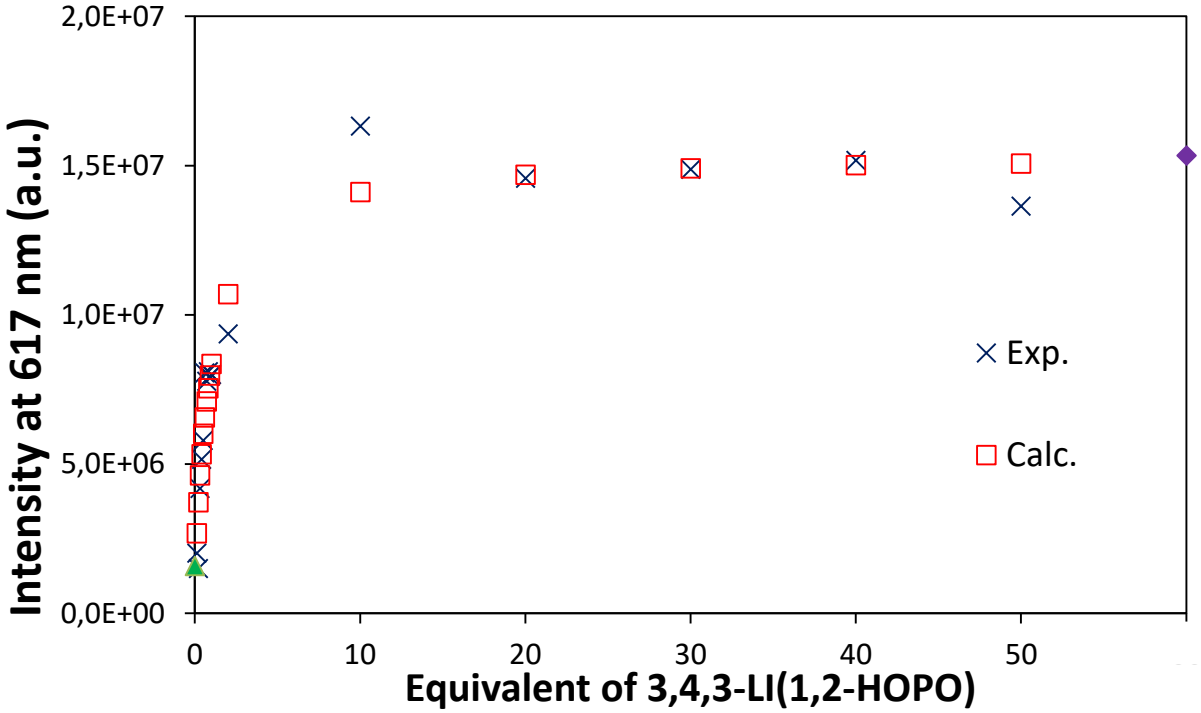

Figure S41. *HypSpec* fit (squares) of data (crosses) from spectrofluorimetric competition titration of Eu.**L** (1. Series) against 3,4,3-LI(HOPO) ([Eu.**L**] = 1.4 µM, [HOPO] from 0 to 70 µM, KCl 0.1 M, 10 mM HEPES, pH 7.4, 25 °C, exc = 325 nm).

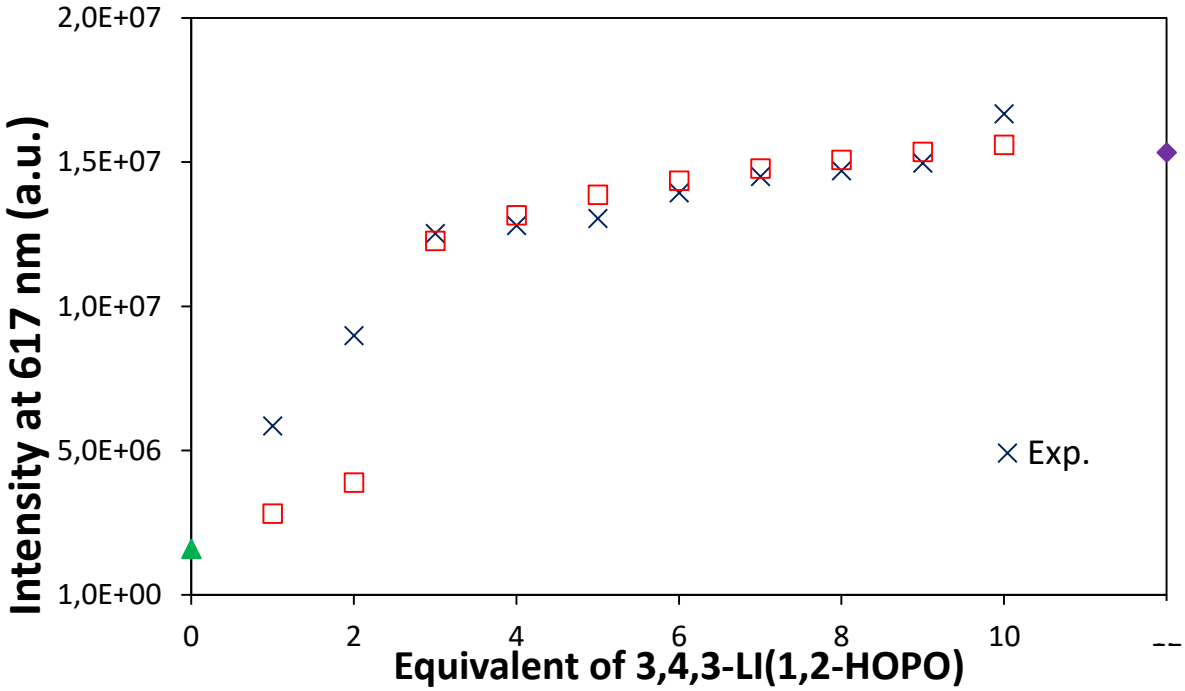

Figure S42. *HypSpec* fit (squares) of data (crosses) from spectrofluorimetric competition titration of Eu.**L** (2. Series) against 3,4,3-LI(HOPO) ([Eu.**L**] = 1.4 µM, [HOPO] from 0 to 14 µM, KCl 0.1 M, 10 mM HEPES, pH 7.4, 25 °C, exc = 325 nm).

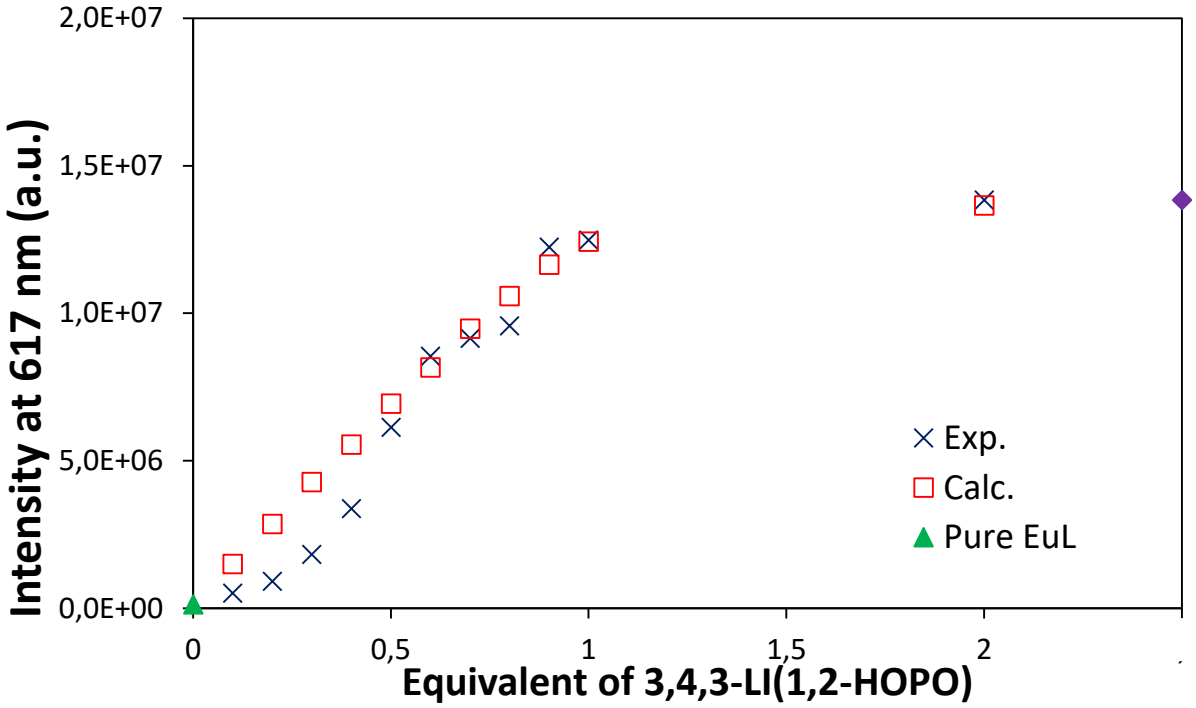

Figure S43. *HypSpec* fit (squares) of data (crosses) from spectrofluorimetric competition titration of Eu.**L** against 3,4,3-LI(HOPO) ([Eu.**L**] = 1.4 µM, [HOPO] from 0 to 3µM, KCl 0.1 M, 10 mM HEPES, pH 7.4, 25 °C, exc = 325 nm).

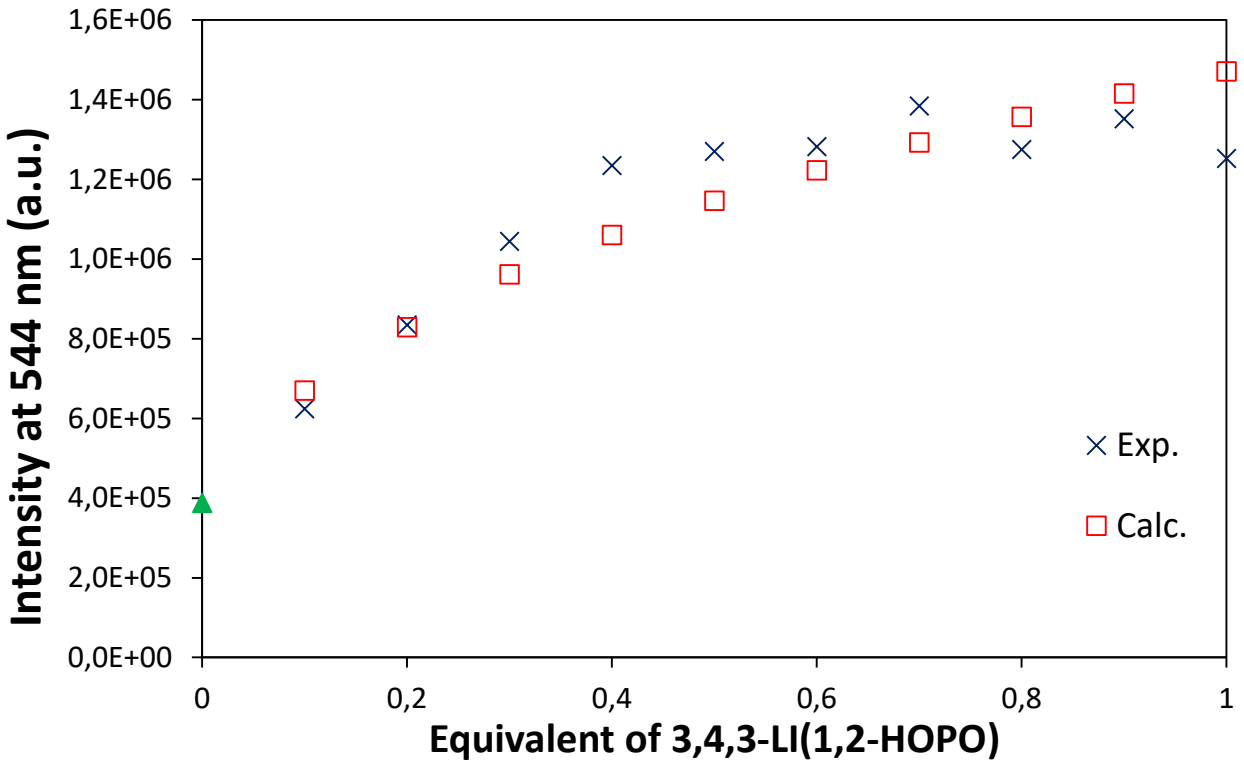

Figure S44. *HypSpec* fit (squares) of data (crosses) from spectrofluorimetric competition titration of Tb.**L** against 3,4,3-LI(HOPO) ([Tb.**L**] = 1.2 µM, [HOPO] from 0 to 1.2 µM, KCl 0.1 M, 10 mM HEPES, pH 7.4, 25 °C, exc = 325 nm).

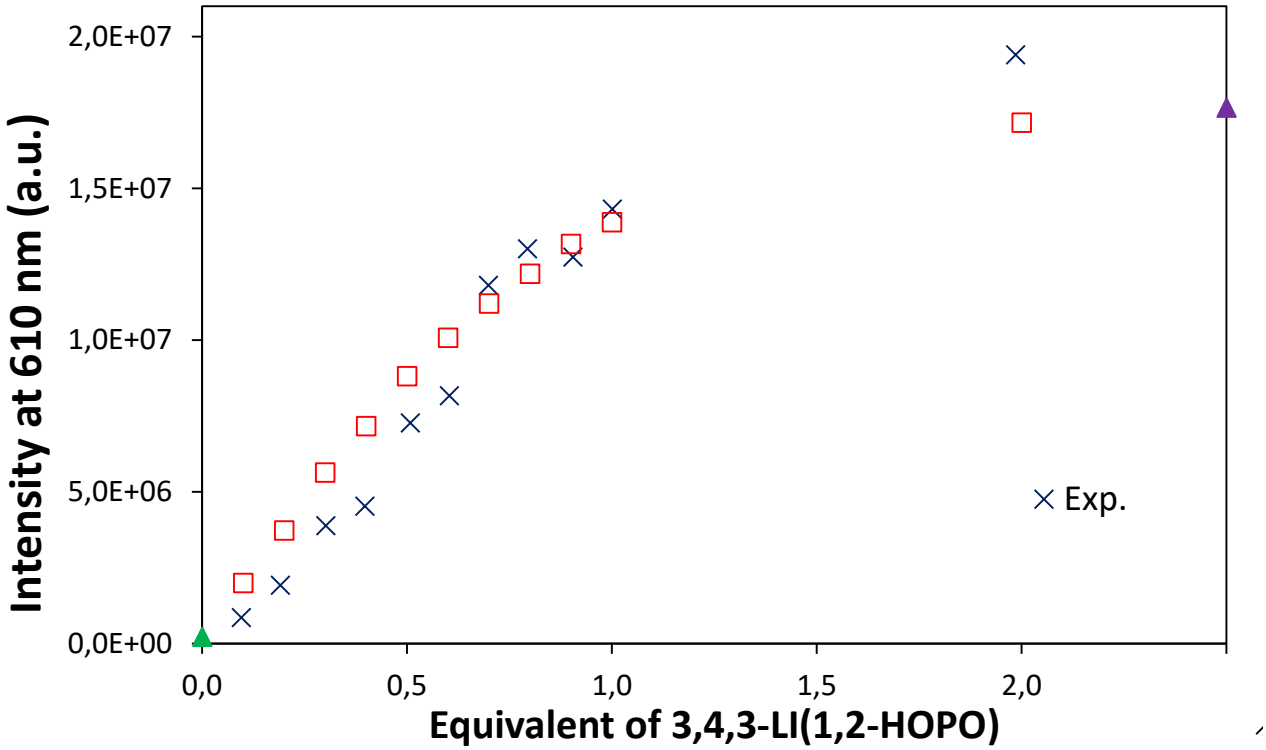

Figure S45. *HypSpec* fit (squares) of data (crosses) from spectrofluorimetric competition titration of Cm.**L** (Series 1) against 3,4,3-LI(HOPO) ([Cm.**L**] = 0.11 µM, [HOPO] from 0 to 0.2 µM, KCl 0.1 M, 10 mM HEPES, pH 7.4, 25 °C, exc = 325 nm).